8 Differential Diagnosis of Breast Cancer by Doppler and Sonoelastography Applied to the Lobar Ultrasonography

Aristida Colan-Georges

8.1 The Differential Diagnosis of the Breast Diseases in the Classical Radiological and Imaging Techniques in Use

The differential diagnosis in the radiological and imaging diagnosis of breast diseases was less performing and with low significance; that was due to the less specific descriptors of the breast findings, by one hand, and to the non-anatomical scanning and interpreting of the pathological findings, neglecting the normal radial lobar architecture of the breast, by the other hand. None of the individual or grouped well-known descriptors of the breast masses in US (upon Stavros [1], and after that included and developed in the US BI-RADS assessment, since 2003 up to 2013 in the fifth edition) have enough specificity in the characterization of a breast malignancy, to avoid the mandatory biopsy in any suspect lesion. No isolated ultrasonographic descriptor, such as shape, orientation, contour, internal structure, and posterior effects, included in the US BI-RADS assessment, can accurately predict a benign or malignant lesion. Mammography cannot differentiate the solid from the fluid lesions, and the microcalcifications used as indirect sign for the positive and the differential diagnosis of breast cancer have low specificity, while their absence cannot completely exclude a breast malignancy.

The most valuable demonstration of the mammographic limits is revealed by the comparative studies including the old screen-film mammography, the newest digital mammography, and the sectional imaging techniques (US, MRI, tomosynthesis). Most comparisons between the two mammographic techniques, including a large study of Sala and col. of a total of 242,838 mammograms (171,191 screen-film mammography group and 71,647 digital mammography group), have demonstrated a false-positive rate higher for the screen film than for the digital mammography (7.6% and 5.7%, respectively; $P < 0.001$) [2]; in addition, the false-negative results are less illustrated.

Digital mammography seems to improve the detection of the breast cancer with 27% in women under 50 years old, compared with the analogue technique, according to the American College of Radiology Imaging Network (ACRIN) that conducted a large Digital Mammographic Imaging Screening Trial (DMIST) in the United States concerning 49,528 women [3]. However, all screening methods are intended in the diagnosis of a cancer as early as possible, neglecting the benign or premalignant lesions; thus the incidence of the breast cancer rested unchanged; moreover,

A. Colan-Georges, M.D., Ph.D.
Imaging Center Prima Medical,
County Clinical Emergency Hospital,
Craiova, Romania
e-mail: aristida_georgescu@yahoo.com;
acgeorges.radiology@gmail.com

D. Amy (ed.), *Lobar Approach to Breast Ultrasound*, https://doi.org/10.1007/978-3-319-61681-0_8

the last recommendation for the breast cancer screening is neglecting the importance of the lesions assessed in the second category of the US BI-RADS. In the meantime, there are not equivalent assessments to the screening US BI-RADS for the symptomatic patients, which are examined without standardized protocols, with some complementary imaging techniques used before the final biopsy because of lack of differential diagnosis.

The classical US was used as a complementary technique of examination in differentiating the solid from the fluid lesions depicted on the mammography; there were used some suggestive descriptors for the benign, indeterminate, and malignant masses upon Stavros. In the classical US, the role of the vascular assessment was underevaluated, limited to the number of poles, size, and course (over three poles for malignant lesions upon 2003 US BI-RADS, with enlargement of the vessels and tortuous course). The sonoelastography was developed the latest, practically after 2003 with the aim to improve the differential diagnosis; it was initially criticized due to the various manufacturers and different scoring or quantitative assessments, and the 2013 US BI-RADS recommends it "with prudency, only if positive results."

The development of the automated breast volume scanning (ABVS) was intended to be used as screening test that is exploring the whole breast, more objective, and with possibilities of computed aided diagnosis (CAD). However, the orthogonal planes remain non-anatomical related to the lobar architecture, the normal breast parenchyma represented by ducts and lobules is neglected, and the coronal plane (plane C) has not a proved relationship with the nipple. Some encouraging studies revealed the value of the ABVS, such as the analysis of Brem and col. [4], which reported for a total of 15,318 women presented to screening mammogram and complementary ABVS, a number of 112 women detected with breast cancer (0.73%): 82 with screening mammography from which 17 were not detected by ABVS and an additional 30 detected with ABVS alone. They concluded the combined techniques were more performing, but that implies double screening techniques, raised costs, and no useful irradiation to 99.27% of women without cancer.

MRI sensibility is superior to any classical method in use, especially in detecting the multiple breast cancer (Fig. 8.1), without possibility to differentiate the multifocal from the multicentric lesions (arbitrarily considered multifocal in the same quadrant and multicentric in different quadrants or at least 5 cm interval). Because of lack of specific descriptors useful in the differential diagnosis, the specificity of the breast MRI is lower, even using the contrast-enhancing curves; thus the number of biopsies is still increased (Figs. 8.1 and 8.2); moreover, the higher costs and the limited availability restrain its use for specific indications [5].

The absence of a pathognomonic descriptor or of an association of descriptors with high accuracy for the positive and the differential diagnosis determined in practice the use of multiple complementariness techniques, with unsatisfactory results. A comprehensive study of Berg and col. from 2012 [5] concerning a total of 2662 women that underwent 7473 mammogram and ultrasound screenings, which detected 111 breast cancer events, illustrated the inconsistency of each technique: 33 cancers were detected by mammography only, 32 by ultrasound only that illustrates the non-concordant diagnosis, just 26 by both techniques, and 9 by MRI after false-negative mammography plus ultrasound; however 11 cancers were not detected by any imaging screening. By conclusion a combined examination with the main techniques in use failed in detection of 9.9% of cases. The sensitivity for mammography plus US was 0.76 (95% CI, 0.65–0.85) and the specificity 0.84 (95% CI, 0.83–0.85). The best sensitivity had MRI and mammography plus US of 1.00 (95% CI, 0.79–1.00), but the specificity decreased to 0.65 (95% CI, 0.61–0.69). The authors concluded the addition of screening US or MRI to mammography in women at increased risk of breast cancer

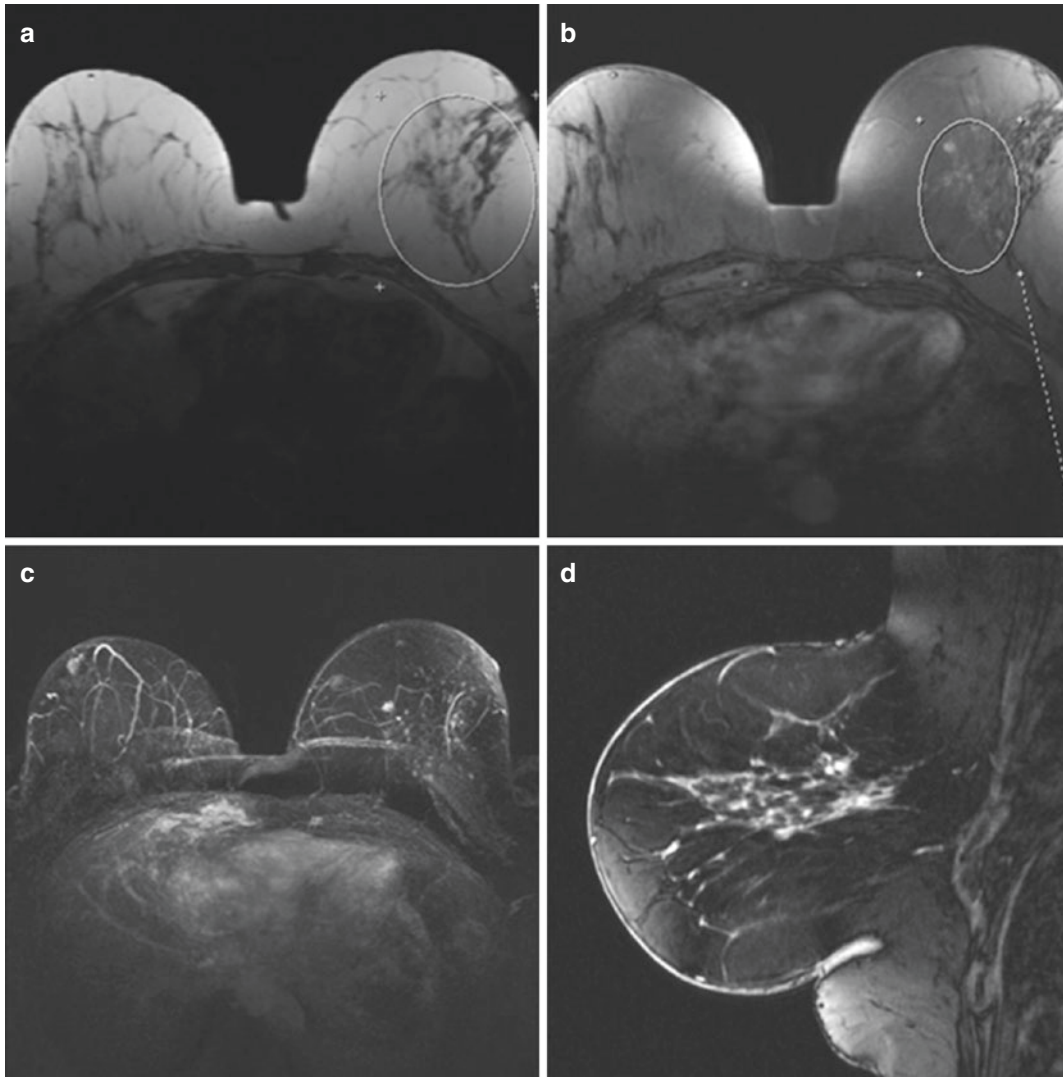

Fig. 8.1 Multiple cancer with small foci in the inner quadrants of the L breast in a 72-year-old patient with previous cancer present the R breast treated conservatory; the lesions present hyposignal T1, with enhancing contrast agent. It is difficult to localize and to precise their multifocal or multicentric type, even using 3D reformatting acquisition or complementary scanning planes (**a**, axial T1WI; **b**, axial T1 Fat-Sat contrast WI; **c**, axial 3D T1 Fat-Sat contrast reformatting image; **d**, sagittal T1 Fat-Sat contrast MPR)

resulted in not only a higher cancer detection yield but also an increase in false-positive findings.

We may conclude the low specificity in the breast cancer detection with isolated or combined radiological and imaging techniques of diagnosis in use is conditioned not only by the inherent technical limits but also by the non-anatomical scanning in arbitrary sagittal, coronal, or oblique plans, in the non-anatomical interpreting of the findings using artificial descriptors mostly borrowed from the mammographic lexicon ("dense" breast, "fibro-glandular tissue," "architectural distortion," etc.).

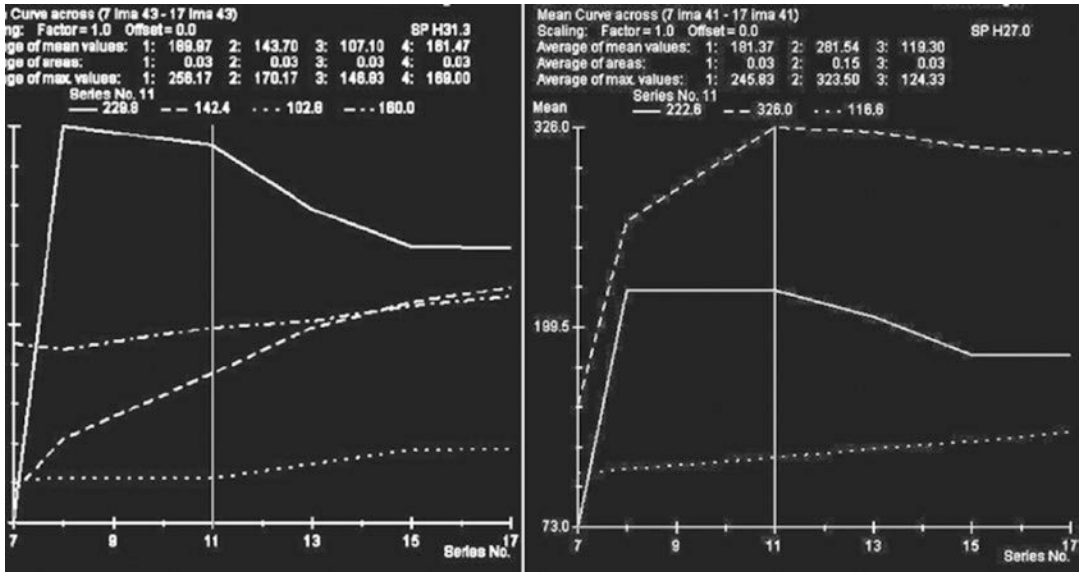

Fig. 8.2 The same case: the specificity of MRI is low, and the contrast-enhancing curves are dependent on the subjective choice of the region of interest (ROI) and on the lesion size; for the smallest, the partial volume artifact is conducting to false-negative diagnosis (*left* image), and for the 5–10 mm lesions, the enhancing curve is suggesting moderate suspect lesion; in conclusion, the global extension of the disease is underestimated

8.2 Significant Descriptors of the Breast Cancer in the New Concept of the Full-Breast Ultrasonography Related to the US BI-RADS Assessment

Last years, more practitioners adopted the anatomical technique of breast ultrasound based on the radial scanning with interpreting of the lobar architecture promoted by Teboul and Halliwell since 1995 [6] and largely spread after 2003 [7]; the lobar view of the breast US corresponding to the gross section of Tot and col. [8] was consequently promoted in all the world by Amy [9, 10], which also had contributions in the conceiving by manufacturers of the long linear probe provided with a water-bag, for a larger radial section without breast deformation and with better visualization of the nipple and superficial layers. These achievements completed with the Doppler examination and the real-time sonoelastography were defined under the concept of "full-breast ultrasonography" (FBU) [11], which allows a comprehensive noninvasive characterization of the breast anatomy and pathology, with better differentiation of the benign from the malignant lesions and with differentiation of some premalignant ductal-lobular changes, unapparent in the other techniques.

FBU realizes a whole-breast mapping using the well-known descriptors used by Stavros and US BI-RADS lexicon but related to the lobar anatomy centered by the ductal-lobular tree. The standardization of the technique made possible the reproducibility and the operator-independent scanning, with better follow-up characterization (Fig. 8.3).

The differential diagnosis of the abnormal findings is more accurate, avoiding unnecessary irradiation and biopsies or other more expansive additional techniques of examinations, and is

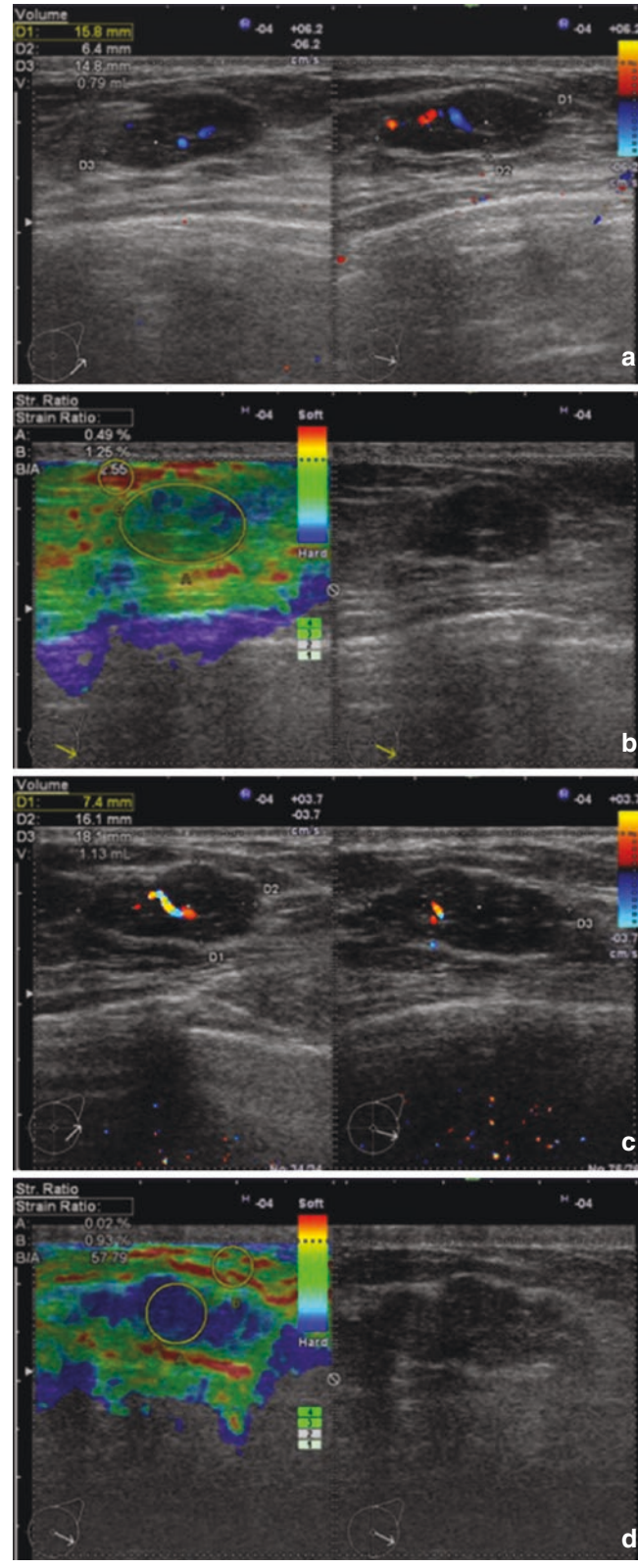

Fig. 8.3 Follow-up examination after 6 months interval of a peripheral lump at L 4:00 locations in a 38-year-old woman demonstrates an increasing volume from 0.79 ml (**a**) to 1.13 ml (**c**), a small increasing of the internal vasculature, increasing of the lobulations on the contour, and a higher stiffness from the score 2 Ueno with the strain ratio up to 2.55 (**b**) to a score 3 Ueno with the strain ratio up to 57.79 (**d**). The lesion assessed by US BI-RADS 4b was referred to conservatory surgery with extemporaneous pathological examination

based on a group of three descriptors: *the ductal connection (present or absent)*, *the vascular characterization by Doppler*, *and the strain evaluation by sonoelastography*.

1. *The ductal connection* is mandatory in the characterizing of the anatomical appurtenance of a lesion: no hypoechoic mass will be suspect of breast cancer without ductal connection. The differential diagnosis includes other malignancies (breast lymphoma, sarcomas) or benign lesions (lipoma encompassed in and buttressed by surrounding dense hyperechoic fibrous tissue, fibrous tissue, others).
2. *Doppler characterization* with new evaluation in the FBU. The 2013 US BI-RADS assessment [12] stated a better role of the techniques of Doppler (absent, peripheral, internal) and SE, but with some limits. Doppler assessment is used for the evaluation of the new formations of vessels in solid tumors, allowing the differentiation of the benign from the malignant masses: for the benign lesions less than three vascular poles, peripheral vessels with arched course, "in basket orientation," with few, thin internal branches or without salient Doppler signal are suggesting; for the malignant masses, more vascular poles, concordant with the tumor size, the enlargement of the vessel diameter compared with those in the normal breast area, and the intratumoral arteriovenous shunts that give rise to flow detected as high-velocity signals, with aliasing similar to other cancers (thyroid, primary hepatocellular, and renal cancer [13–15]) were demonstrated. The intratumoral microvessel density is an important prognostic marker of survival in breast cancer [16, 17]. The use of contrast-enhanced US (CEUS) increased the sensitivity and specificity to 100% in the differential diagnosis of benign/malignant primary breast lesions according to Kedar [18]; moreover, CEUS of the breast had high accuracy for the assessment within 2 mm of pathologic tumor size according to Van Esser [19].

   In our experience, all these vascular descriptors are useful in FBU in the differential diagnosis of benign/malignant breast lesion; in addition, the anatomical scanning uses the vascular assessment especially in demonstrating the multifocal ductal carcinoma with intralobar distribution by intraductal spreading following the lowest pressure; the number of salient vessels and their size and velocity is proportional with the main tumor size and decreases as the size of the secondary (the nearest) or tertiary (distant) malignant foci increases. Moreover, all descriptors of the new formation vasculature used in the US BI-RADS lexicon are more or less subjective and should be completed by one of the most important, objective, and with pathognomonic value in the differential diagnosis: the incident angle of the plunging artery described by Kujiraoka et al. [20]. Any cancer type focal, multifocal, or multicentric will be found with at least one vascular pole with incident angle of the plunging artery; thus the scanning in the radial and antiradial plane is mandatory (Fig. 8.4); except for the diffuse increased vasculature in the lobar or the diffuse cancer (inflammatory breast cancer), and for the lactating breast, which can be differentiated adding the SE. (Figs. 8.5 and 8.6).
3. *The breast SE*, despite the EFSUMB guidelines, is still unstandardized, because of different manufacturers and of various scoring systems; this is the reason two follow-up SE performed with different systems may be impossible to evaluate for any benign or malignant evolution of a breast lesion. However, the real-time SE upon the Ueno (Tsukuba) scoring is best correlated with the US BI-RADS assessment (Fig. 8.7).

The sensibility of the SE is quite high for the differential diagnosis of the infracentimetric cancers that do not demonstrate malignant descriptors, the sentinel satellite lymph nodes, the local recidivism, and the malignant scars. SE in malignant less vascularized lesions is more sensitive than breast contrast MRI (Fig. 8.8); however, the diagnostic value of the SE alone must not be overestimated, because of the low specificity for

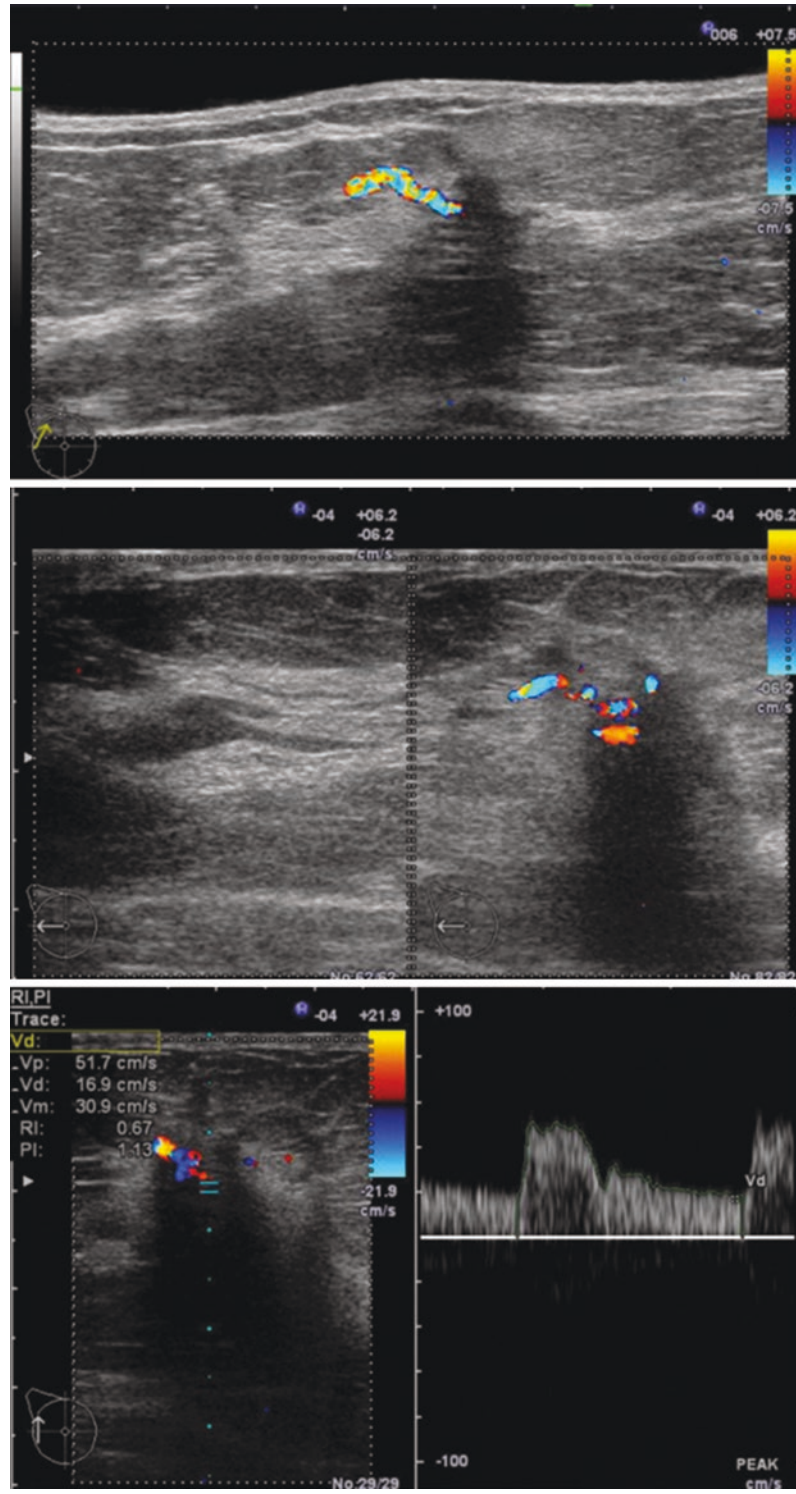

Fig. 8.4 Malignant type of new formation vasculature in ductal echography: the hypoechoic lesion with ductal connection demonstrates large, tortuous vessels, with aliasing and an incidental angle of the plunging artery after Kujiraoka et al. [20]

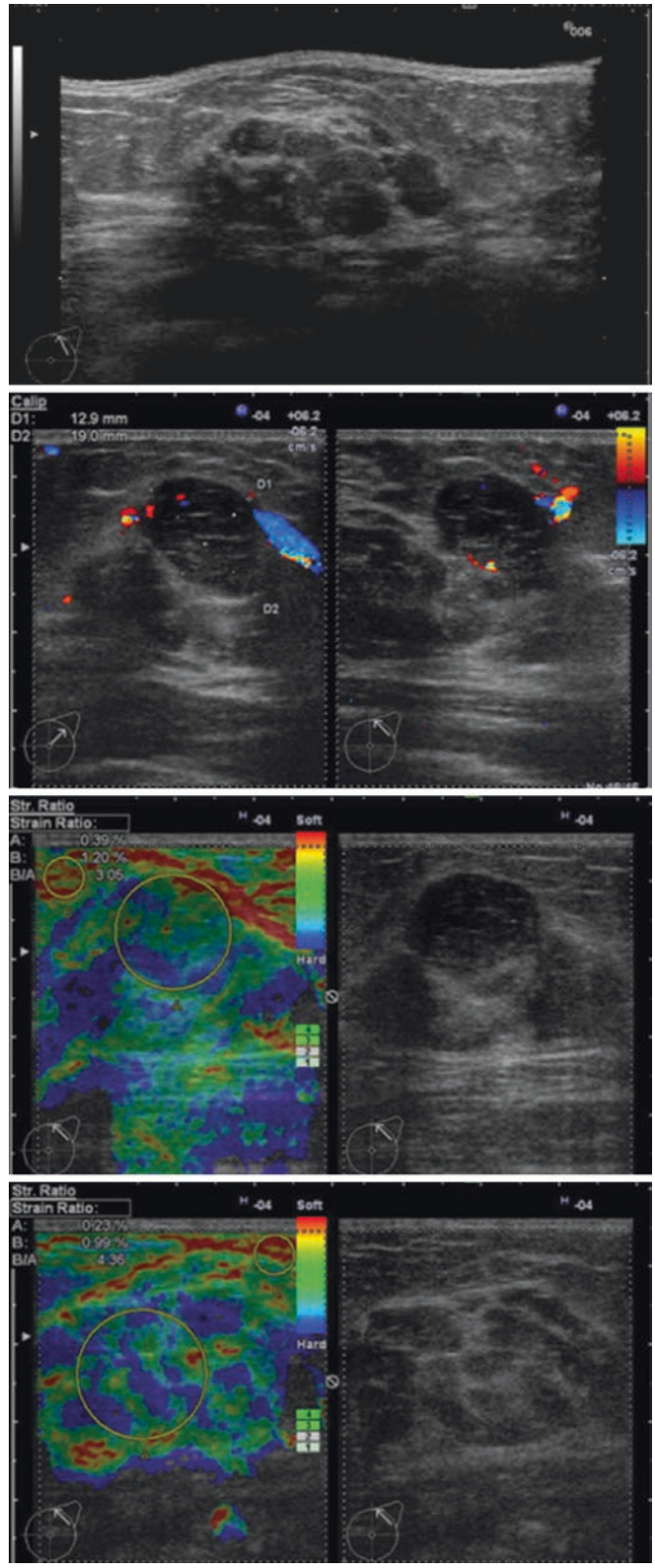

Fig. 8.5 FBU demonstrates a multifocal cancer type ILC, in a 59-year-old patient: the hypoechoic masses with ductal connection of various size and shape are grouped in the left axillary glandular prolongation, with pathological new formation vasculature and high strain

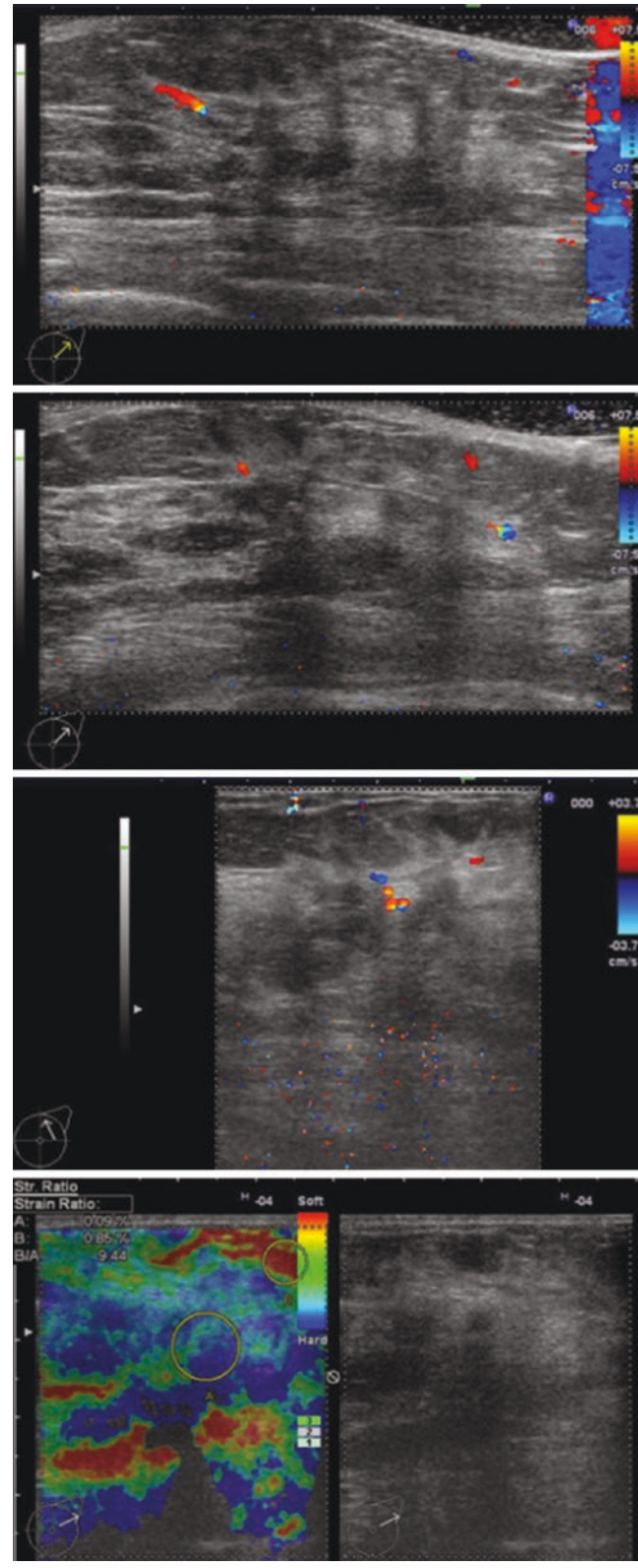

Fig. 8.6 Comparative FBU demonstrates a lobar type of an IDC in a 68-year-old patient: the small hypoechoic lesions with acoustic shadowing, new formation vasculature, and high strain are connected by the ductal tree and distributed in a lobar volume (radial and antiradial scans), suggesting the intraductal spreading way of the malignancy (multifocal breast cancer)

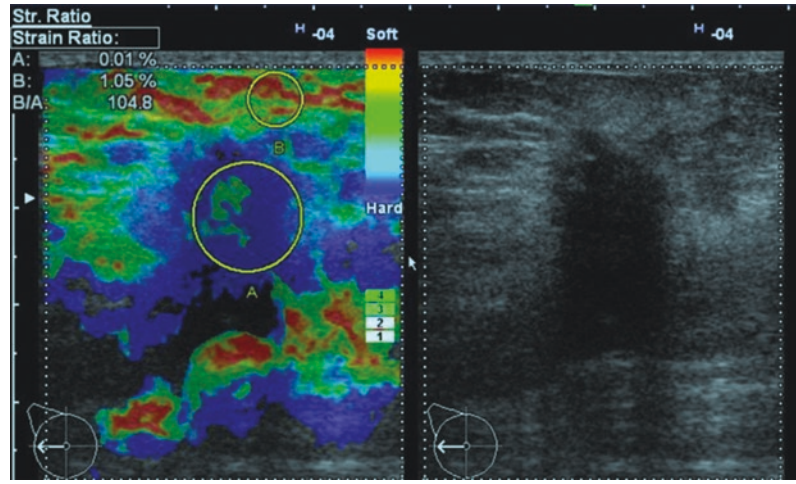

Fig. 8.7 The SE aspect of an IDC with halo in 2D US and acoustic intense shadowing demonstrates a score 5 Ueno and high strain with FLR over 100.0, with posterior artifact, concordant with the malignant microcalcifications visualized on the mammography—BI-RADS 5 category

the score 4–5 Ueno, found in malignant lesions as well as in benign ones (scars, sclerosing adenosis, suture granulomas, etc.), which will be further detailed.

FBU improves the differential diagnosis of the breast cancer because of integration of the anatomical view with the vascular findings and the SE scoring; this integration of the SE was already recommended by users of the classical US, for avoiding some false-positive and false-negative diagnosis [21]. In the anatomical radial scanning, SE was proved the best tool in the differential diagnosis of the inspissated duct or cyst that may mimic solid lesions in 2D US but illustrate a BGR or summation-BGR score [22].

Some solid findings such as a nonvascularized fibroadenoma with hypoechoic aspect may have a score 2 or 3 Ueno, while an atypical mucinous, medullary, or papillary carcinoma type illustrates benign 2D US features with more or less increased new formation vasculature and a score 4 Ueno.

FBU may diagnose not only the nodular type of breast cancer but also the lobar and the diffuse cancer, based on the illustration of the pathological ductal lobar tree; the pathological correspondence of the FBU findings is superior, the radial scanning allowing the differential diagnosis of the multifocal cancer (in the same lobe, possible in different quadrants) from the multicentric cancer (in different mammary lobes, possible in the same quadrant), being proved the lobes may overlap, but they have no ductal interconnections.

8.3 Differential Diagnosis of the False-Positive Cancers Using the FBU: Breast Cancer and Pseudo-malignant Lesions

There are two types of errors reported in the diagnosis of the breast cancer in the classical US: the false-positive and the false-negative findings [23].

The false-positive findings result in falsely high BI-RADS category assignment such as lipoma encompassed in and buttressed by surrounding dense hyperechoic fibrous tissue, fibrous tissue and scar with acoustic shadow, inspissated echogenic ductal secretions, ducts with fluid-debris level or fat-fluid level, fibromicrocystic dysplasia, etc.

It is generally assumed the fatty breast is easier to examine by mammography, but it is difficult to diagnose in US, because both fatty layers and malignant lesions are hypoechoic, and some benign lesions could mimic malignancies in the 2D US in the arbitrary transverse and sagittal scans. The false-positive results published by the classical US were determined by the non-anatomical scanning and interpreting of the breast images and by the inconsistent use of the

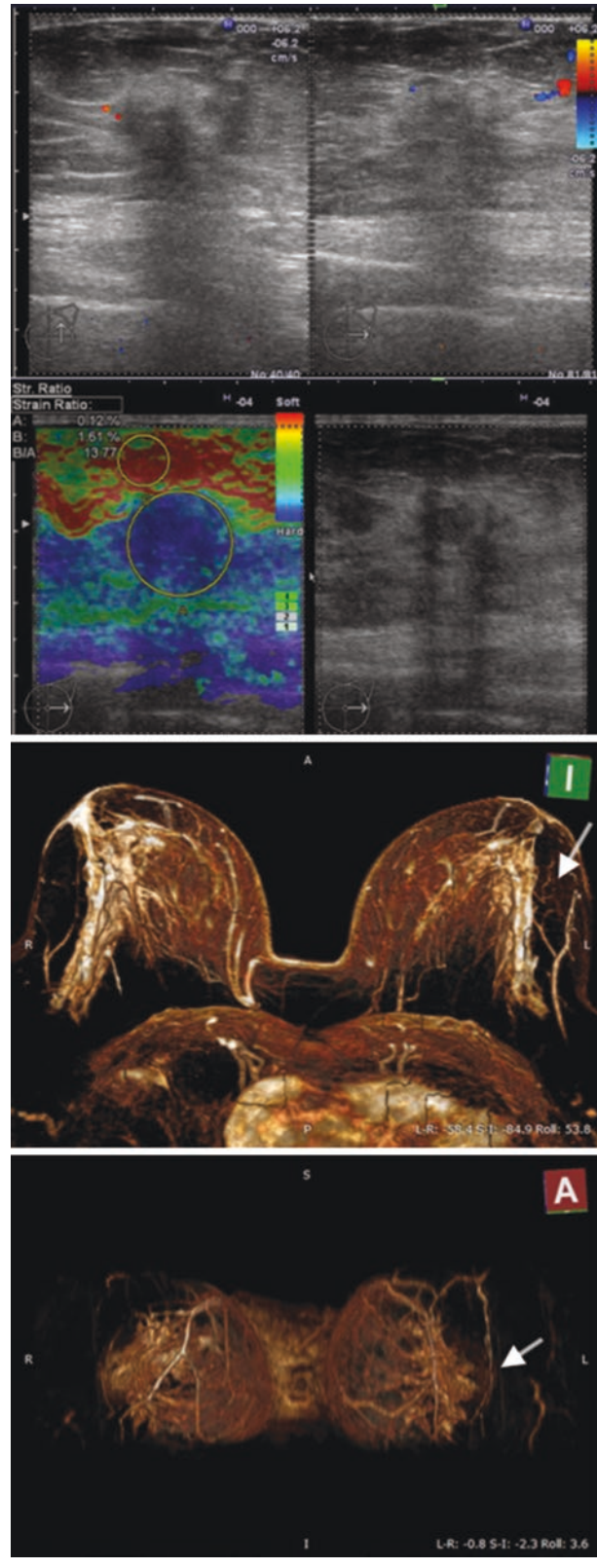

Fig. 8.8 Atypical findings in a 57-year-old patient, which presented a lump in L 3:00, with mammographical assessment BI-RADS 0 and inconsistent findings in 2D US (isoechoic aspect but with acoustic shadowing, thin peripheral new formation vasculature but with incident angle of the plunging arteries) and without pathological significant lesions or enhancement curves in MRI examination (not shown); the SE demonstrates a score 5 Ueno, and a second look of the MRI with 3D reconstruction of the T1 contrast-WI confirms an asymmetrical discrete enhancement in the same area (arrows in the axial and frontal views). The US-guided biopsy confirmed breast malignancy

Doppler characterization; the unsatisfactory results published about SE were related to its use as an independent method of examination that was compared with the 2D US alone. By consequence, it is assumed SE cannot differentiate the benign scars, the fibro-microcystic dysplasia (FMCD), and the calcified fibroadenoma from malignant lesions, all of them presenting low elasticity.

The radial scanning used in FBU allows a better differential diagnosis by illustrating the ductal connection of the breast cancer, while the lipomas are located either in the pre- or retromammary fatty tissue or between some branches of the ductal tree. Moreover, all hypoechoic findings with acoustic shadow which may have increased stiffness at SE, such as scars, diabetic fibrous mastopathy, and fibro-microcystic dysplasia, do not illustrate new formation vasculature with suspect descriptors (incident angle of the plunging artery, tortuous enlarged vessels, high velocity with aliasing).

The inspissated ducts or cysts and other segmental ductal abnormalities (ducts with fluid-debris level or fat-fluid level) have benign findings in FBU, with absence of suspect vasculature and a benign score at SE, type score 2, 3, BGR, or complex BGR.

Better results of the SE in the differential diagnosis are related to some recommendations for the technique of acquisitions:

- For the real-time SE, we should avoid a strong compression (range 5–6) that would determine false-positive images, most tissues looking hard.
- A small area of the surrounding tissues do not allow a good evaluation of the lesion stiffness, but a large region of interest (ROI) from the skin to the ribs offer a large scale of elasticity from the softest (fat) to the hardest (bone).
- The evaluation of the stiffness of a pathological finding must not be resumed to a unique measurement, but we should note an average of 3–4 qualitative and quantitative (FLR) sonoelastographic evaluation for each lesion, in radial and antiradial scans; the quantitative results may be expressed in strain ratio for the Hitachi devices and in kilopascal (kPa) or m/s for the shear wave elastography.
- In characterizing the benign lesions, it is useful to determine the highest strain ratio (FLR) or stiffness measured as pressure units (kPa), expressed in the report as "high elasticity/low strain of up to…," rather than the mentioning of a unique precise value; similarly, for the malignant assessment, it would be suitable to mention the lowest value of the quantitative measurements, to reassure the surpassing of the cutoff value: "low elasticity/high strain of FLR over…" or "low elasticity of over …kPa."

As illustrated, we mention an analyze of a series of 810 FBU, including randomly symptomatic and screening patients, which identified 149 cancers in 132 patients; from all, we had three false-positive cases of breast cancer, all of them in the beginning of this series, determined by the insufficient training; the diagnosis was based mainly on the DE with the presence of the malignant BI-RADS descriptors reinforced by the overestimated diagnostic value of the real-time SE of scored 4 or 5 Ueno but neglecting the Doppler less salient signal; in two cases, the surgical biopsy was performed, and the pathological result précised fibro-microcystic dysplasia, and the third case presented a chronic over infected deep hematoma, confirmed by FNA biopsy. The secondary analize of the images noted absent/reduced vasculature of suspect lesions, with benign acute angle of the plunging vessels, and a complex SE with increased stiffness areas combined with a summation/complex BGR score [24].

Fibro-microcystic dysplasia represents a pseudotumoral form of the cystic disease, considered by some authors as a premalignant lesion, but of lower risk for developing malignancy upon others (0.3% according to Venta et al. [25]), comparing with the ductal and lobular atypical hyperplasia; its importance in the differential diagnosis is done by the similar findings with many breast cancers on mammography, classical breast US, SE alone, and MRI. The fibro-microcystic dysplasia appears in the DE as a pseudo-malignant

mass with hypoechoic aspect, connected to the ducts, with irregular/spiculated borders, acoustic shadowing, but without significant new vasculature on Doppler. Sometimes such small nodules are found in the site of the terminal ductal-lobular specific units (TDLU), considered as the initial site for the developing of any mammary lesion, either benign or malignant [26]. In our experience, there were no cases of breast cancer (without chemotherapeutic or radiotherapeutic treatment) without Doppler salient abnormal signal. Moreover, fibro-microcystic dysplasia presented a summation-blue-green-red (BGR) score at real-time SE, similar to the fluid structures over 4 mm diameter, with a low to medium FLR concordant with the benign lesions (Figs. 8.9, 8.10, and 8.11). The fibro-microcystic dysplasia represents the key in the differential diagnosis for the SE, but it was not well interpreted in the literature, even by the promoters of the real-time SE, which did not describe the summation-BGR score (we have chosen this term because the strain of the sum of the cluster of immeasurable cysts was similar to those of a unique cyst of appropriate volume).

The strain ratio of the fibro-microcystic dysplasia is not characteristic, according to the "hard" ROI selected inside the lesion; the selection of the whole area of BGR complex or summation type generally presented a strain ratio

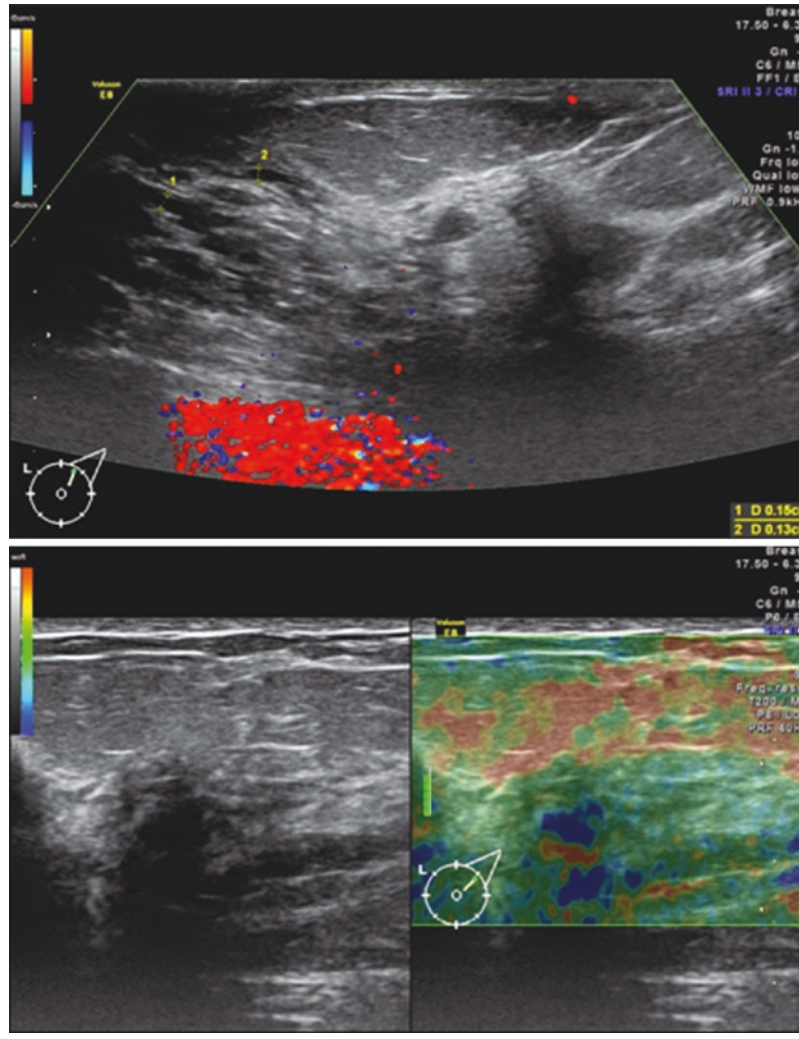

Fig. 8.9 FBU in a 56-year-old patient illustrates central ectasia and a pseudo-malignant peripheral lesion with ductal connection, with ill-defined, hypoechoic, and spiculated borders, with acoustic shadowing and taller than wide; the negative Doppler and the BGR-type score made the differential diagnosis in this fibro-microcystic dysplasia

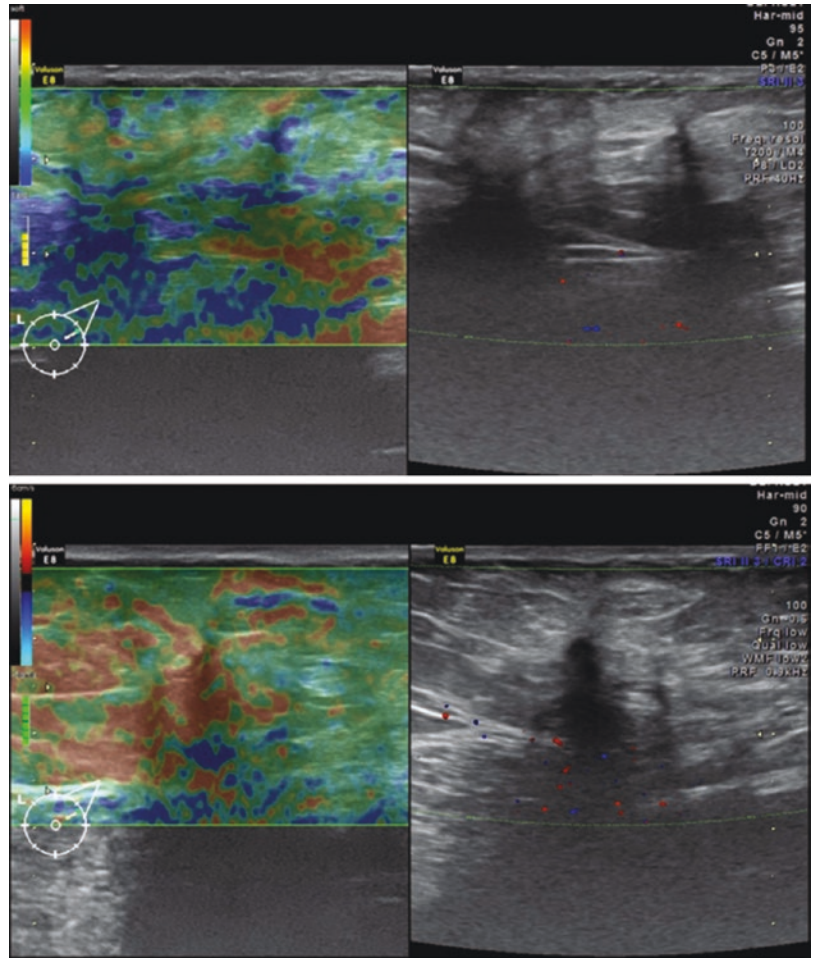

Fig. 8.10 FBU in a 69-year-old patient with lobar malignant findings both at mammography and 2D US; the negative Doppler and the BGR-type score suggest a fibro-microcystic disease, concordant with the biopsy

(FLR) of <4.70 considered for the cutoff value [22] and conducted to the final diagnosis as a benign lesion with low risk to develop cancer, assessed by US BI-RADS 3 category.

Fibrocystic dysplasia is a frequent finding, considered by some authors as a form of the "sick lobe" [27, 28]; it is easy to diagnose in the limited phenotype, with few measurable transonic cysts, or in the diffuse phenotype of the Reclus disease, but the diagnosis is more difficult in the inspissated cysts and in the nodular fibro-microcystic lesions (Fig. 8.12). In a series of 819 patients, we found 282 (34.43%) cases with fibrocystic dysplasia, of which 79 (9.6%) cases included the nodular type presenting a clinical pseudotumoral more or less painful aspect [22]; FBU illustrated unique or multiple lesions with multicentric or multifocal distribution, sized between 0.5 and 3 cm. There were frequently associated (macro) cysts, ductal ectasia, in few cases ductal papilloma, benign nodular hyperplasia (fibroadenoma), or diffuse ductal or lobular hyperplasia but rarely was present a breast cancer (Fig. 8.13).

Ductal ectasia in non-breastfeeding women is present in many painful breasts, both in benign and malignant diseases. Nipple discharge and especially bloody nipple discharge is considered having a benign etiology in 80% of cases (duct papilloma, duct ectasia) and rarely may be malignant (duct carcinoma). The usual radiological and imaging differential diagnosis is difficult due to many factors:

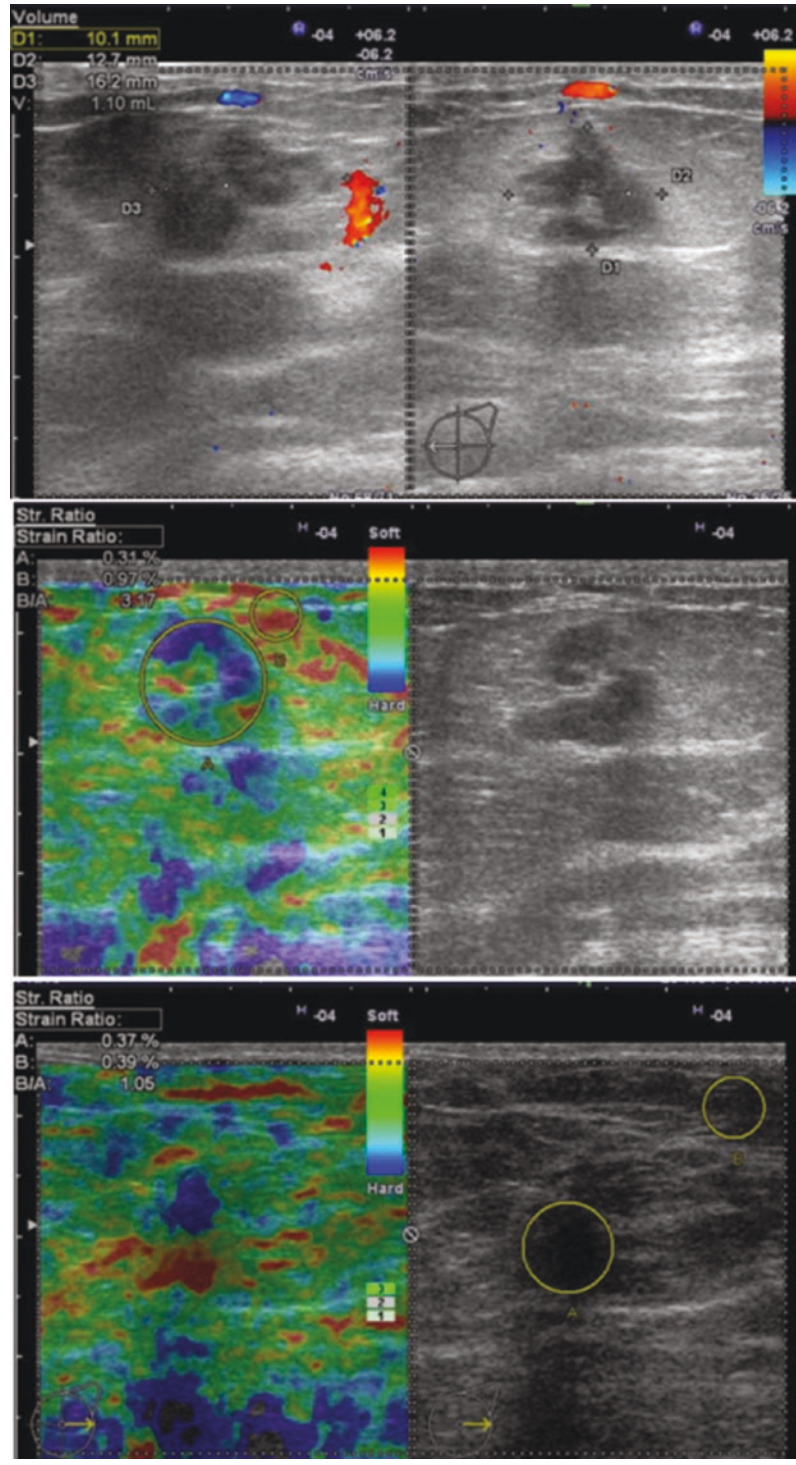

Fig. 8.11 FBU in a 60-year-old patient with pseudo-nodular infracentimetric findings grouped in a TDLU location; there are some peripheral salient vessels in Doppler examination; the hypoechoic structure and the irregular shape with variant orientation are unspecific, but the BGR score of the SE is suggesting for the nodular fibro-microcystic dysplasia

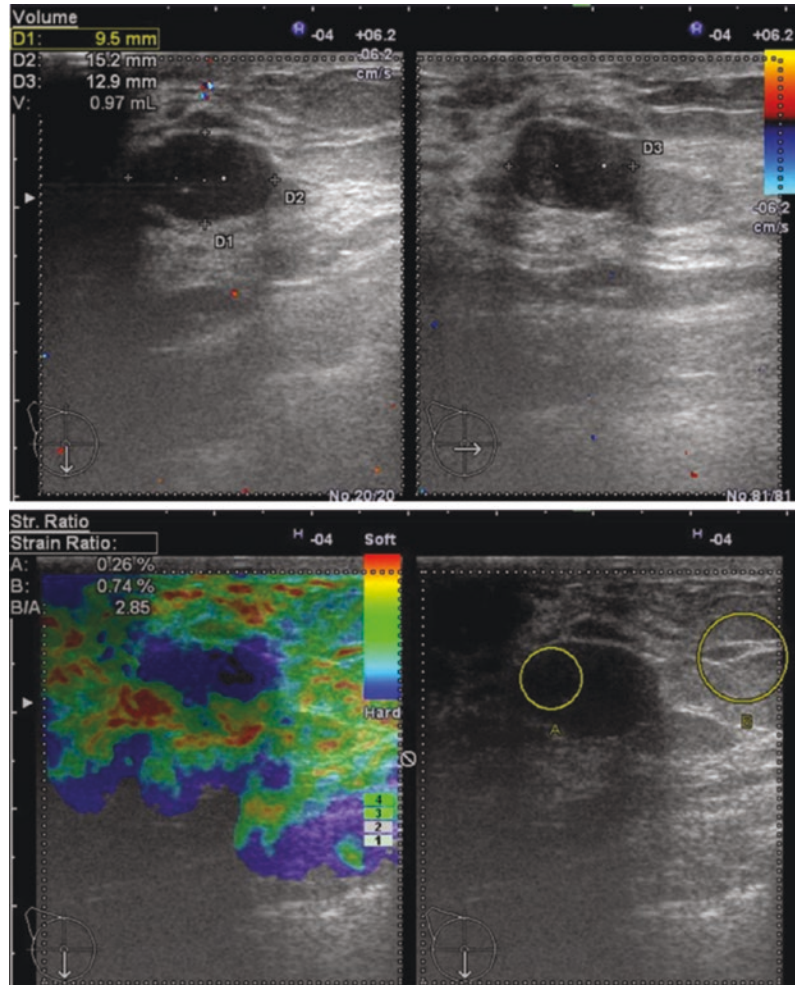

Fig. 8.12 Inspissated cyst, the differential diagnosis with a solid mass: the absence of any Doppler signal together with a BGR score, whatever the protein content of the cystic fluid

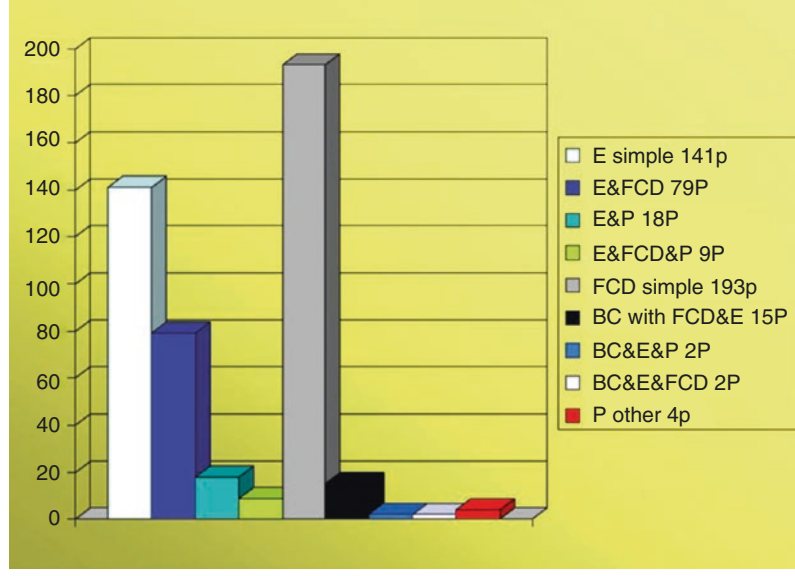

Fig. 8.13 Distribution of the secretory changes: E simple = ductal ectasia without other abnormalities; FCD = Fibrocystic dysplasia, including FMCD; P = papilloma; BC = breast cancer (upon [22])

- The mammography and the tomosynthesis cannot visualize the normal and abnormal ductal walls, but sometimes the intraductal microcalcifications localize and orientate the diagnosis.
- Mammography may demonstrate intraductal calcifications in bloody nipple discharge both in chronic galactophoritis and in comedo DCIS; frequently the mammography underestimates the extension of DCIS because it cannot detect the ductal walls without microcalcifications [29].
- The radiological galactography is an invasive technique, with uncertain results.
- The classical US does not explore the ductal tree.
- The ABVS and MRI, despite their multiplanar techniques, have low resolution and may incidentally illustrate segments of thickened ducts.

FBU differentiates the chronic galactophoritis inside the group of ductal ectasia and demonstrates the absence of a pathological periductal vasculature in the presence of a chronic infection with various types of staphylococcus (*S. aureus*, *S. albus*, *S. epidermidis*, and so on), *E. coli*, proteus, and *Candida albicans* (sometimes found equally in acute mastitis of lactating women) [30] (Fig. 8.14). The differential diagnosis of the chronic galactophoritis is made with the physiologic (breastfeeding) or pathological hyperprolactinemia (galactorrhea) that demonstrates a diffuse increased breast vasculature or hyperemia (Fig. 8.15) and with segmental ectasia with localized (peri-)ductal vasculature associated with papilloma or breast cancer.

In addition, the real-time SE is useful in the differential diagnosis of duct ectasia whatever the fluid density, presenting in thin and middle ductal ectasia the score 1 Ueno-like (green walls with red lumen) and in large, pseudo-cystic ducts the BGR score; the ductal papilloma and DCIS may demonstrate the score 2 and 3 Ueno (Fig. 8.16).

The chronic no puerperal breast infections are frequent but rarely diagnosed and treated; usually the nipple discharge or the fine-needle aspirate is intended only for the cytological tests, but the diagnosis of these infections is important because they represent the main cause of the painful breast without skin changes that could be treated; moreover, galactophoritis is frequently associated in the florid stage with ductal hyperplasia and in the final stage with ductal atrophy and nipple retraction, mimicking carcinoma or Paget disease [22]. These chronic infections may lead to the disfigurement of the breast secondary to repeated operations and to an empiric antistaphylococcal treatment [30]. Their differential diagnosis by FBU allows conservative treatment avoiding unnecessary biopsies or the surgical procedures.

Ductal thickening differential diagnosis implies specific descriptors for different etiologies. Ductal hyperplasia may be either diffuse or segmental; the diameter of the ducts is increased, but this thickening must be correlated with the patient age and the individual breast ductal pattern: in the young woman, 1.5–2.5 mm is considered normal ductal thickness, while in the postmenopausal woman, the normal ducts are ranged <1.0 mm. The differential diagnosis is made by the preserving of the central hyperechoic line representing the virtual lumen in duct hyperplasia, while in intraductal papilloma, the thickening of the ducts is done by a central mass surrounded by thin walls. Ductal hyperplasia has a score 1 or 2 Ueno-like (Fig. 8.17), duct papilloma has a score 2 or 3 and low FLR, while DCIS appears with loss of the ductal central line sign, increased thickness, hypoechoic walls sometimes with hyperechoic granular echoes (without certitude of microcalcifications in the absence of the mammography), with at least a score 3 Ueno and salient vasculature (Fig. 8.18).

Lobular hyperplasia may appear as isoechoic micronodules connected to the ducts, usually in a TDLU location; the size of few millimeters must be interpreted according to the age and the physiological condition; there are not salient local Doppler signal, and the SE demonstrates a score 2 Ueno for the glandular area (terminal ductal-lobular structures and glandular stroma). FBU allows the differential diagnosis with the <5 mm breast cancer, which has always a ductal connection, and can

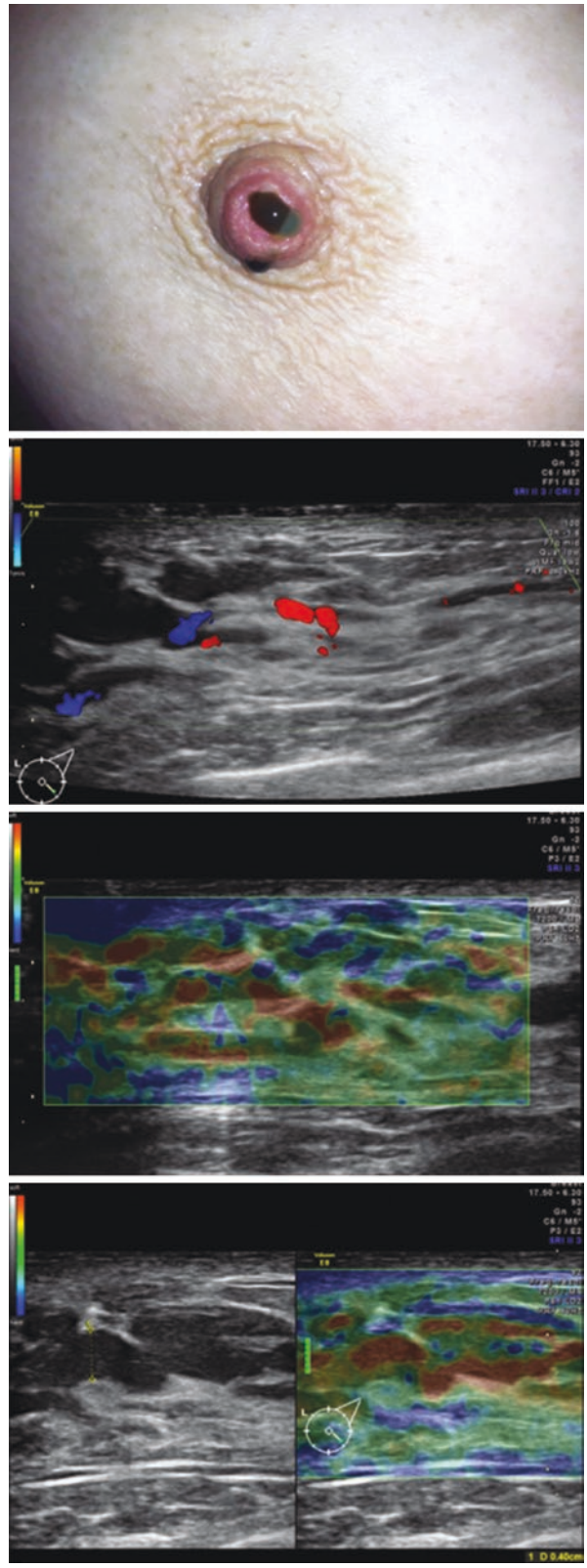

Fig. 8.14 Bloody discharge in a 35-year-old patient with duct ectasia overinfected with *Staphylococcus haemolyticus*; the color of the secretion may be different in the same breast, there are no skin changes, and the ductal content may be hypoechoic or with fluid-fluid level; the SE demonstrates a score 1 Ueno for the thin ecstasies or BGR for the largest ones

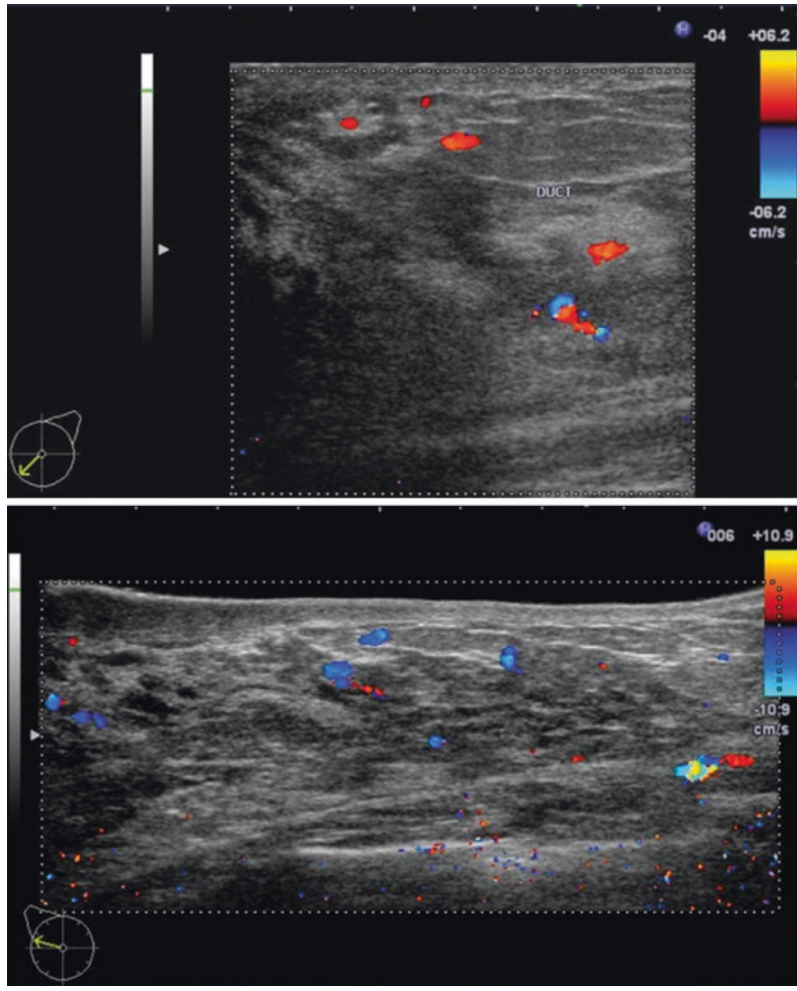

Fig. 8.15 Hyperprolactinemia (*upper* image) and lactating breast (*lower* image): reduced pre- and retromammary fatty tissue, dense parenchyma with small duct ectasia, and the pathognomonic increased diffuse breast vasculature; no breast edema or skin thickening found in acute mastitis

miss the acoustic shadow; the shape and the borders may be confusing of benign type, but usually there is a salient new formation vasculature which represents the most important tool in the differential diagnosis; the SE shows a score 3 or 4 Ueno for the small cancers, and its value is just complementary.

Suspect lesions <5 mm are not palpable and they are difficult to locate and characterize by mammography or breast MRI; a short-time US follow-up may be useful before the decision of biopsy. In our experience, a suspect lesion of 3.5 mm diameter with unipolar new formation vasculature doubled the dimensions and reached new vessels in 2-month interval, and the pathological report confirmed a DCIS. In other cases, a peripheral lobular hyperplasia in a postmenopausal woman, more hypoechoic than the surrounding parenchymal structures, with blurred stroma, without Doppler signal and with medium

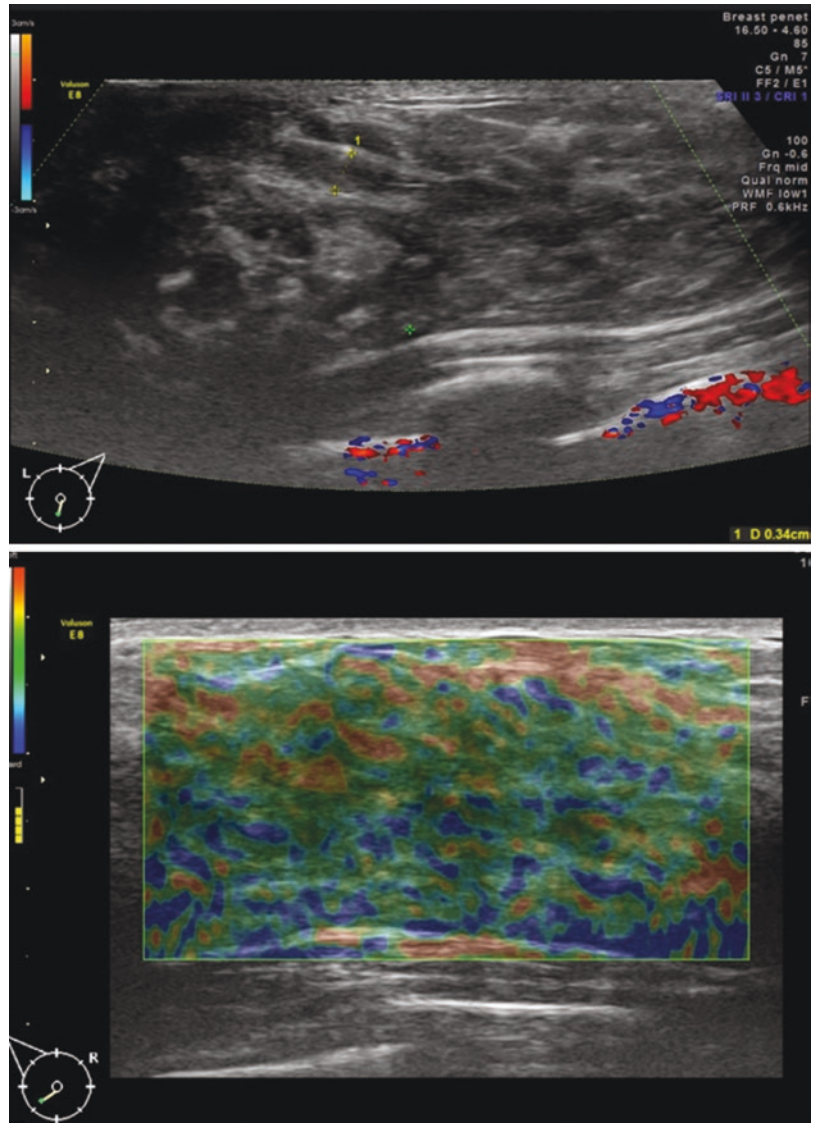

Fig. 8.16 Ductal hyperplasia in a 22-year-old patient with mastodynia: ductal thickness up to 3.5 mm associated with loss of the central line sign, without Doppler signal, and the SE with a global score 2 Ueno

FLR values, developed in a 9-month interval a multifocal lobular carcinoma with salient new formation vasculature and a score 5 Ueno for the glandular area.

The false-positive diagnosis of the benign hyperplastic scar as a local recidivate can be overruled in the FBU by the analysis of the duality vasculature and strain: in the early postoperative follow-up, the benign scars may illustrate thin peripheral reparatory vessels without important fibrosis, while in a late stage, there are no more vessels, and the strain is increased.

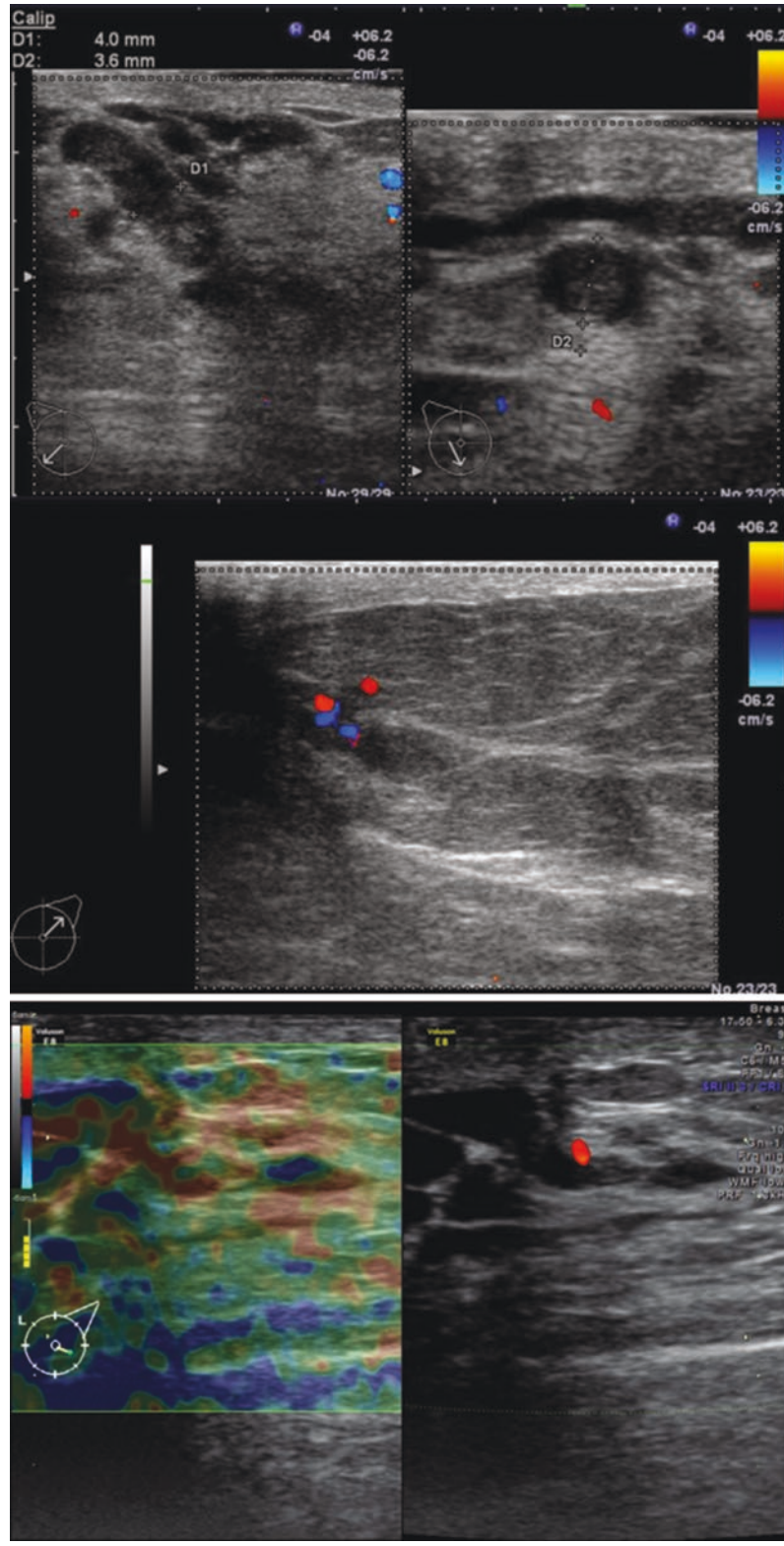

Fig. 8.17 Ductal papillomas

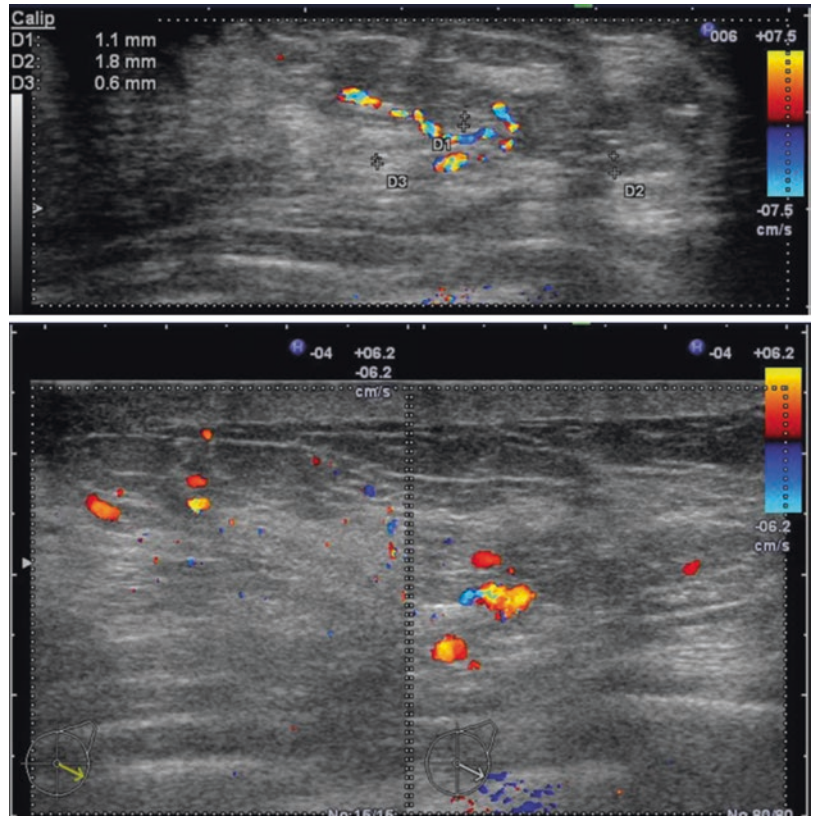

Fig. 8.18 Relapse of a DCIS in L 4:00 after conservative surgery a year before followed by radiotherapy; skin thickening and increased vasculature in the areas with inhomogeneous ductal thickening, illustrated using a long linear transducer (*upper* image) and a short high-frequency transducer (*lower* image) with composed double screen

8.4 Differential Diagnosis of the False-Negative Cancers Using the FBU: Breast Cancer with Pseudo-benign Appearances

The group of *false-negative findings* results in a false BI-RADS category assignment falsely too low, missing the diagnosis of the breast cancer. There are many different causes of false-negative diagnosis invocated in the classical US:

- Technical reasons: volume averaging in the near and in the far field, gain too low, time-gain curve too flat, and isoechoic nodules without high-frequency coded harmonics
- Some pathological specific conditions:
  - Lack of the posterior effects of colloid nodules with incomplete volume characterization
  - Papillary, medullary, and mucinous carcinomas with pseudo-benign features
  - Impossible visualization in US of the most malignant microcalcifications
  - Small carcinomas that lack specific suspicious features
  - DCIS with extensive necrosis
  - Diffusely infiltrative lesions such as classic infiltrating lobular carcinoma
  - Intracystic carcinoma

These reasons are correct, but they are applied to an incomplete US breast examination, limited

to the possibilities of the 2D US, without mentioning of the Doppler and SE more specific aspects; some technical limits may be improved, but the sensibility of the US exam will not increase, and the false-negative diagnosis will persist because of the orthogonal axial and sagittal scanning, with risk of missed regions to the examination.

FBU aspect of the pseudo-benign findings in the gray-scale examination, such as colloid nodules and papillary, medullary, and mucinous carcinomas, will demonstrate the ductal connection of a mass and a salient new formation vasculature with suspect descriptors: incident angle of the plunging artery, tortuous course, enlarged lesional vessels, and higher velocity of the tumoral vessels with aliasing as compared with the normal flow in the rest of breast vasculature; complementary SE will add information about the strain alteration.

The differential diagnosis with other findings presenting salient abnormal vasculature includes the real benign lesions: some infected cysts with pericystic inflammation, the abscesses, infected hematomas, or ruptured implants demonstrate vascular changes; in these cases, SE offers a differential diagnosis presenting benign scores. Breastfeeding diffuse hyper-vasculature may be easily differentiated by SE from the acute mastitis and the malignant mastitis: the strain of the subcutaneous fatty tissue and of the mammary lobes is normal in hyperprolactinemia, the fatty tissue is inversely more stiff than the glandular structures in benign mastitis, and the stiffness is significantly increased for the glandular lobes in malignant mastitis [11]. These differential descriptors were neglected in the classical US because of lack of correlation of US available tools with the breast physiology and the lobar anatomy.

There are other cancers without microcalcifications or without stromal reaction with its characteristic spicules, with false-negative diagnosis in mammography and MRI. In these cases, the presence of the malignant new formation vasculature with increased flow and possible arterial-venous shunts may be characterized by Doppler and it corresponds to the MRI dynamic contrast curves, which are suspect for malignancy when depict rapid enhancing (pick) with plateau (done by new vessels with enlarged diameters) or washout (arterial-venous shunts).

Other differential diagnoses for pseudo-benign findings, such as diffuse infiltrating lobular carcinoma, DCIS, small carcinomas without acoustic shadow, peritumoral halo, or spiculated borders, are easy to perform using the mentioned three elements: the ductal-lesion connection inside the mammary lobe, the Doppler with malignant aspect, and SE with increased strain.

In the cases with previous mammography and important diagnosis discordances, a targeted short-term control FBU seems reasonable instead of a painful biopsy that has high risk of false diagnosis up to 25% in the literature [31–33]; a dynamic volume measurement of the suspect lesion (radial × antiradial × anterior-posterior diameter) with vascular and elastographic comparative characterization is more useful for the differential diagnosis than the hypoechogenicity, the long-axis/short-axis ratio, the posterior effects, or the stromal reaction (Figs. 8.19 and 8.20). The differential diagnosis in cases of simultaneous multiple lesions or of atypical cancers with discordances between the radiological and imaging techniques is based on the duality new vasculature-low elasticity with a score 4 or 5 Ueno and a high strain ratio (with the cutoff value of 4.7 for the Hitachi devices) (Figs. 8.21, 8.22, and 8.23).

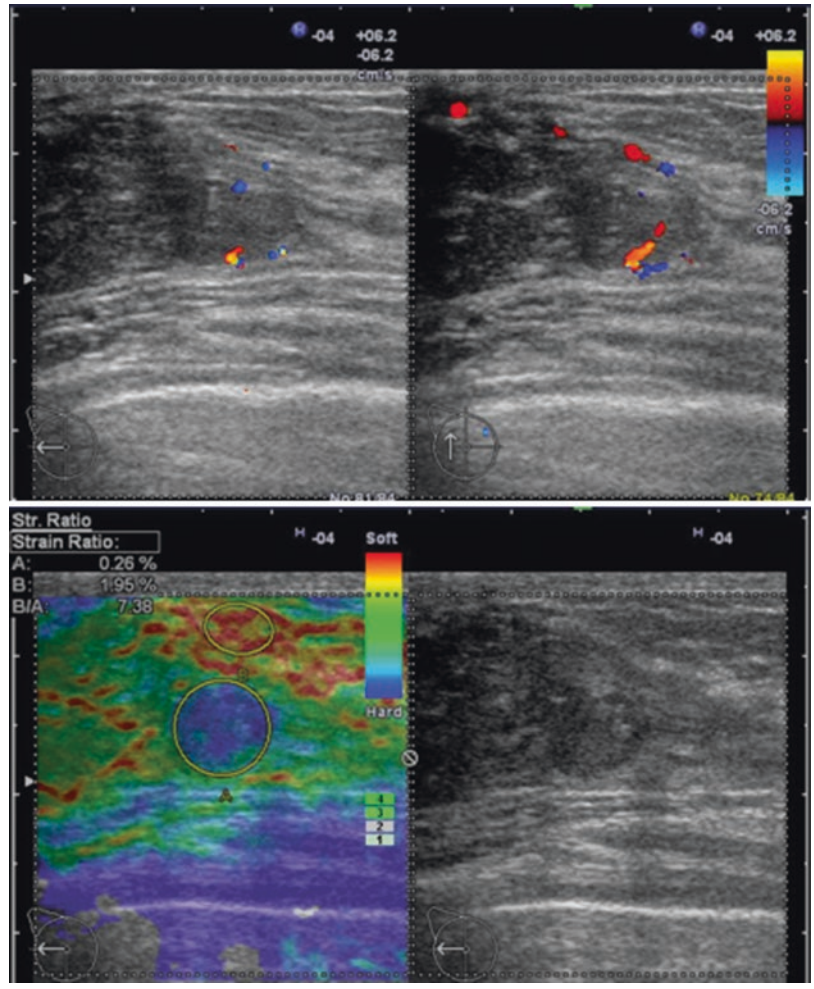

Fig. 8.19 Infracentimetric breast cancer at R 9:00, in a 37-year-old woman masked in 2D US by the dense breast parenchyma; the new formation vasculature and the score 4 Ueno with FLR over 7.00 make the differential diagnosis

8.5 Differential Diagnosis of Breast Scars

The differential diagnosis of the breast scars is possible by FBU not only in the conservative surgery but in cases with radical surgery-type mammectomy or mastectomy and breast cosmetic surgery (mastopexia, breast reduction, and breast reconstruction).

The scars may appear in US as linear or irregular hypoechoic area related with the skin scar, with more or less acoustic shadowing. The benign scars usually do not illustrate suspect vasculature, and the SE is unspecific with various strains, according to the etiology and the time of evolution; some cases illustrate suture granuloma with pseudo-nodular lesions, seroma and hematoma with BGR score, and architectural distortion in conservative treatments but with low strain, sometimes associated with nearby benign breast lesions (cysts, ductal ectasia or hyperplasia, fibroadenoma) (Figs. 8.24 and 8.25).

The radial scars are not related to surgical scarring and are rather a constructed image on the mammography, which illustrates a volumic projection in a plane, than a true pathological

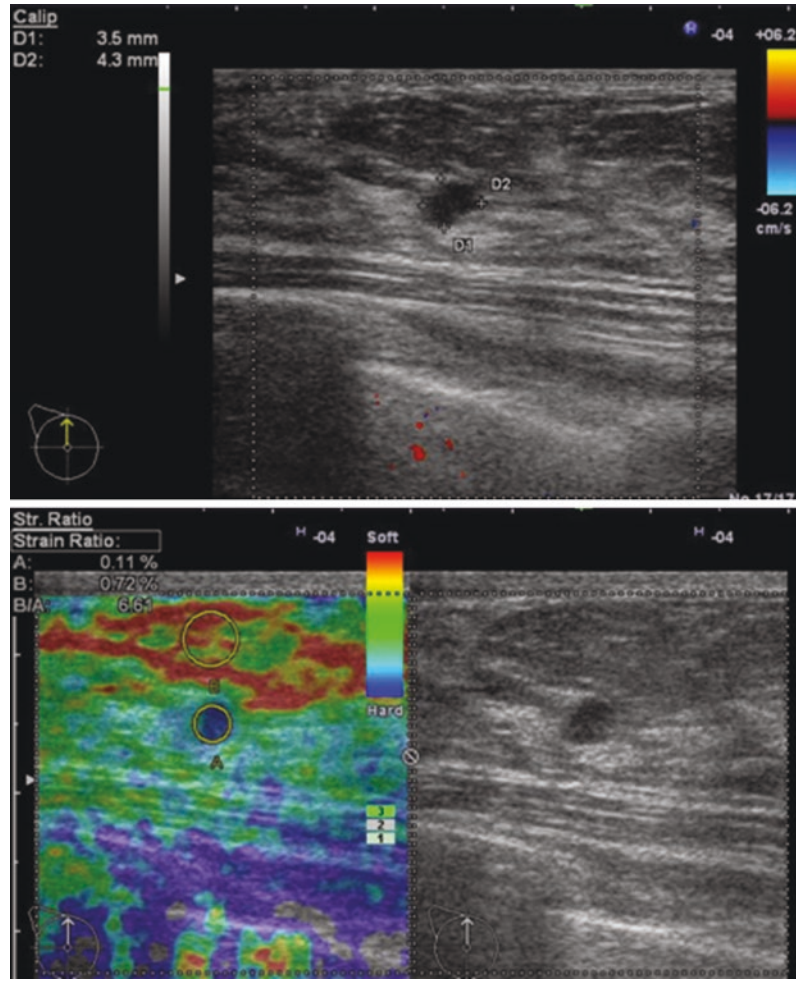

Fig. 8.20 Less than 5 mm breast cancer misdiagnosed in Doppler 2D US as cluster of microcysts; SE with a score 4 Ueno and FLR up to 6.60 recommended a short-time follow-up, with doubled lesion size and proven DCIS after 3 months; this case may explain some "interval" cancers

mass; in the classical US, they were described somewhere different characters, such as disturbed architecture of the surrounding breast parenchyma, ill- or well-defined mass with round or oval shape, acoustic shadowing, etc. Despite its fibrous core and a score 3 or 4 Ueno, there are no suspect new formation vasculatures in the so-called radial scar examined by FBU, and the benign aspect does not justify the recommendation for biopsy. The histopathological aspect confirms a benign lesion that contains hyperplastic tissue cells and a central fibrous core, with radial extension of tubular structures that have two rows of cells, epithelial and myoepithelial, justifying the spiculated peripheral borders. The radial scar is not palpable, and radiologically it is mimicking infiltrating carcinoma; some authors consider the risk of developing malignancy two times greater than in the normal population, but others affirm there is not a higher risk of radial scars than of fibrocystic disease, and there are no differences in the frequency of radial scars in women with and without breast cancer [34].

The "malignant scar" is a recent term used for the local recurrence of a breast cancer in the area of the surgical scar, to differentiate it from other local recurrences of the disease in the same

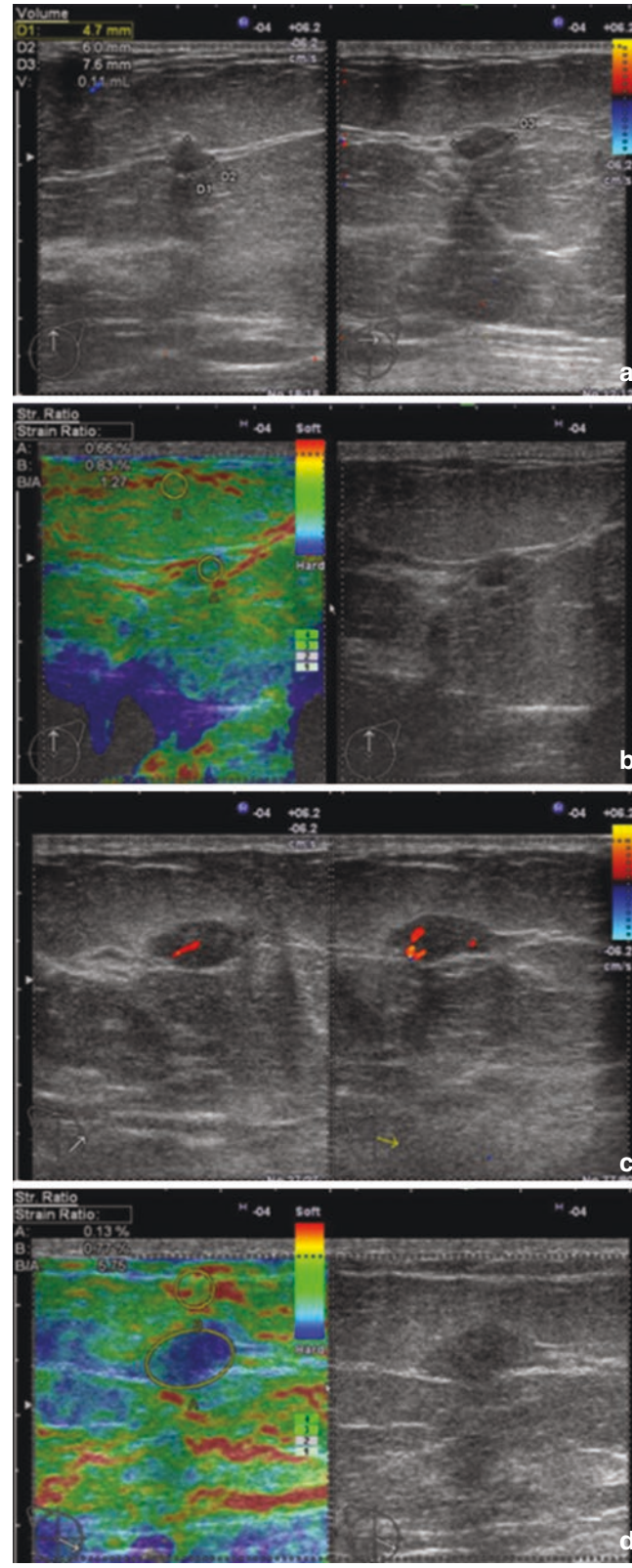

Fig. 8.21 Differential diagnosis of a benign infracentimetric nodule in L 12:00 (**a** and **b**), with a similar size breast cancer in R 4:00 (**c** and **d**), in a 42-year-old patient; the ductal connection and the 2D US findings are similar with benign descriptors upon Stavros and ACR BI-RADS assessment, but there are significant differences in Doppler signal and strain evaluation; the discrepancy between the 2D benign and the final FBU diagnosis is suggesting for atypical breast cancer of mucinous or medullary type

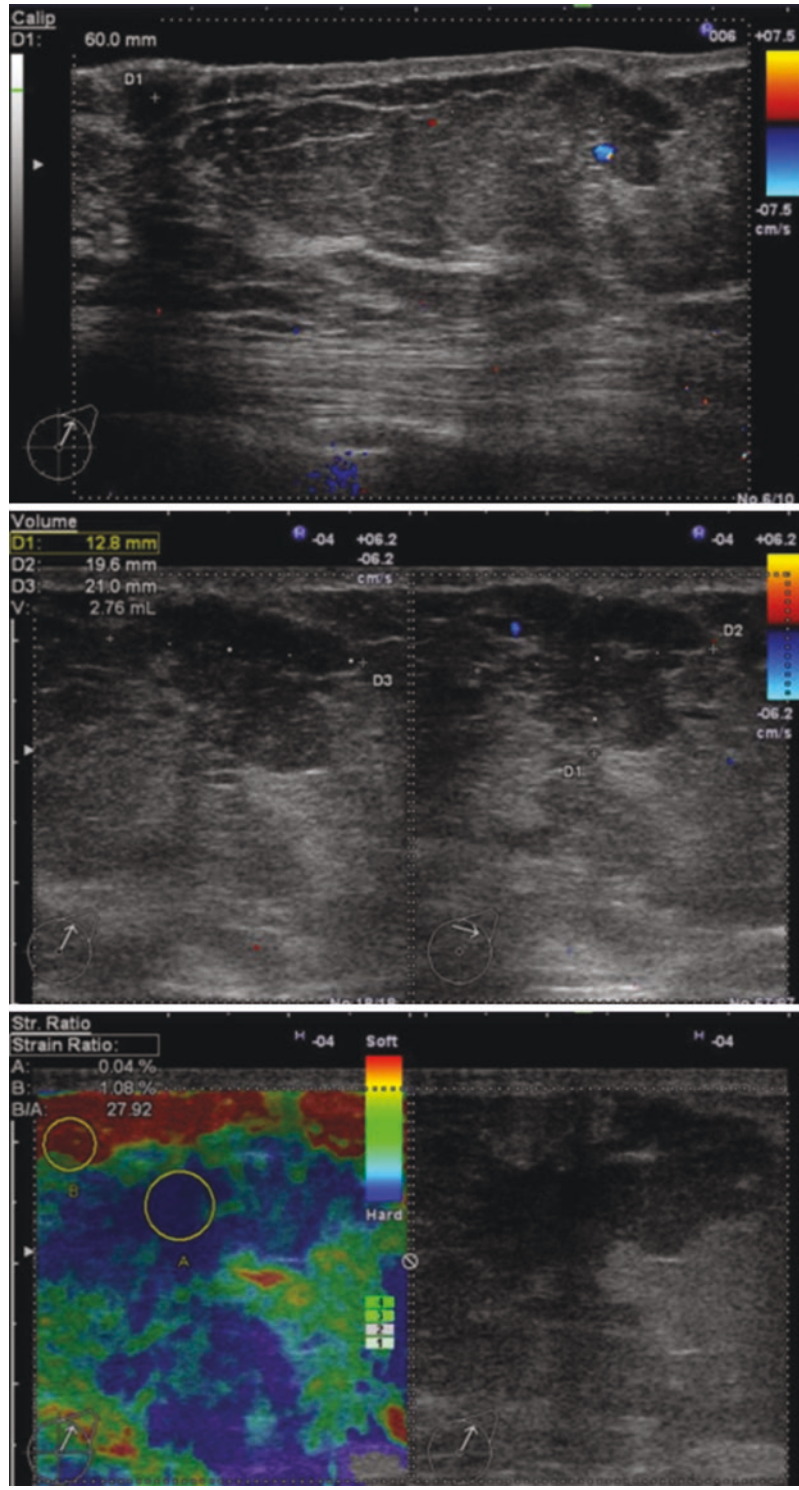

Fig. 8.22 FBU in an atypical breast cancer with 4 years evolution in L 1:00, in an 87-year-old patient: benign features (posterior acoustic enhancement, wider-than-tall and low-but-salient Doppler signal) and malignant descriptors (multi-lobulated borders, eccentric shadow, low elasticity with a score 5 Ueno, and FLR up to 27.92). The differential diagnosis should include fibro-microcystic dysplasia (SE summation-BGR score), trauma-contusion, hematoma (history, normal skin, complex BGR score), diabetic mastopathy (history, biological tests), lymphoma, etc. The pathological report confirmed mucinous cancer, not very rare in elderly women

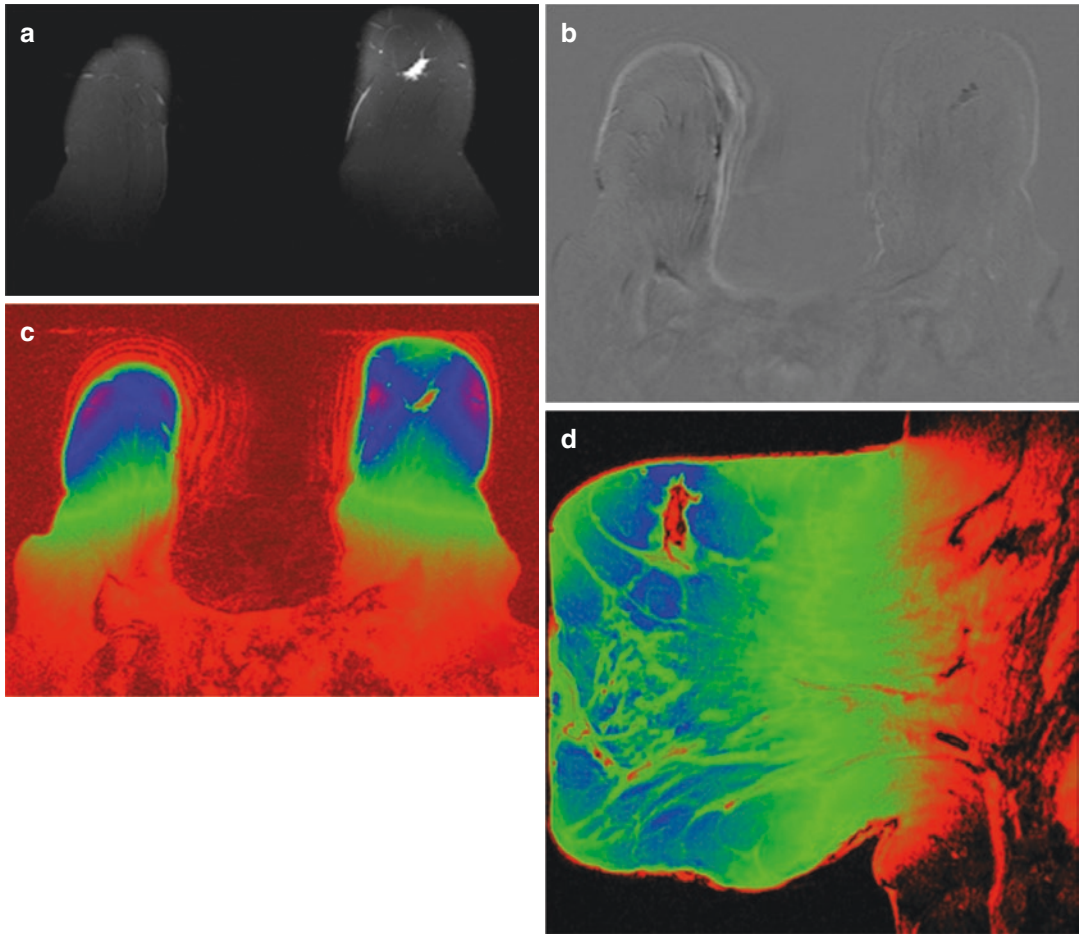

Fig. 8.23 Atypical breast cancer—the same case: MRI examination has a false-negative diagnosis, with hypersignal T2 Fat-Sat WI (**a**) and without contrast pathological enhancement (**b**) T1 Fat-Sat contrast subtraction WI; however, the retrospective color mapping of the contrast sequences (**c**—axial and **d**—sagittal views) was more useful in the characterization of the pathological mass, proving a reduced contrast enhancement undetected by the usual protocols

breast after conservative surgery, or distant from the scar in the small parts of the anterior hemi thorax after radical treatment, which can be considered as local metastases [35]. The earlier diagnosis of a malignant scar by the follow-up care during the complex treatment of the breast cancer is possible by US completed with Doppler and SE each 6 months during the first 3 (5) years and once a year after that (Fig. 8.26); in special cases, further imaging examinations for detection of distant metastases (CT, MRI, PET-CT) will be performed after individualized schedule.

The secondary malignancies closed to the surgical scar in the conservative treatment or in the ipsilateral breast are not rare, between 10% and 15% in the literature [36], and may be explained by the non-anatomical technique of excision-type lumpectomy or segmentectomy with arbitrary limits or even by incomplete excision of the mammary lobe containing the tumor, with possibility of missing some intraductal secondary foci of tumor dissemination. Because at least in the initial stages breast cancer develops inside a lobar structure, due to the complete distinction between the lobar ductal trees, the whole lobe must be excised according to the "sick lobe theory" [27, 28]; thus a new technique of conservative surgery was developed beginning with 1988 and perfected by Enzo Durante [10], with developments by Giancarlo Dolphin and others, which begin with the dissection of the sentinel lymph node, continue by mobilization of the nipple-areola complex for reducing scar formation, and finish with the

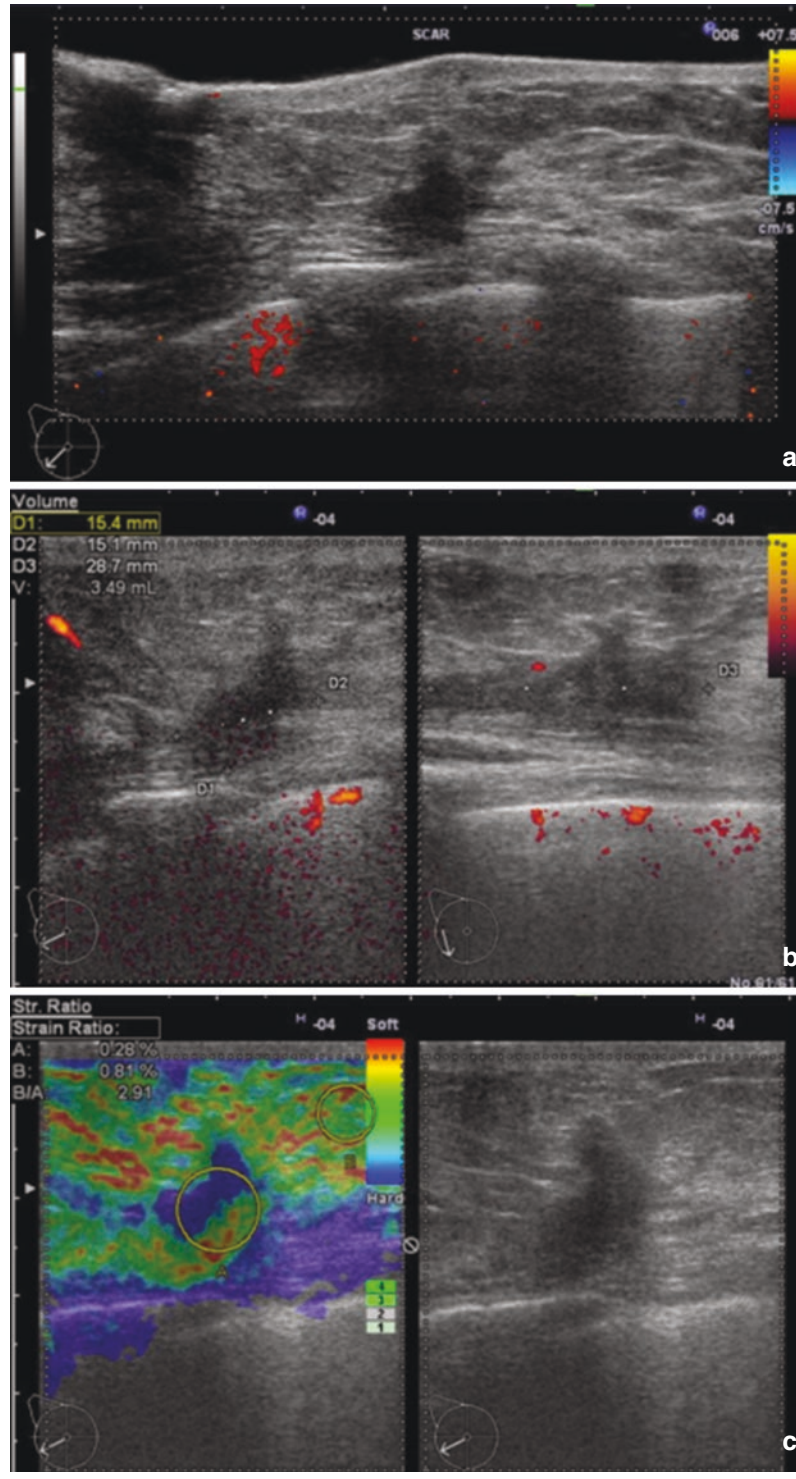

Fig. 8.24 Pseudo-malignant aspect of a chronic seroma after conservative surgery of breast cancer in a 58-year-old woman; seromas are frequent findings after a classical "segmentectomy," which does not respect the lobar anatomy

complete excision of a single affected lobe up to the nipple [37]. The removed lobe is then examined by US in the surgical room, and the presence of the tumor inside is verified. As results there are less 0.3% cancer relapses after Dolphin with conservative surgery of minimal but complete excision of the sick lobe; because the vascular supply is related to the

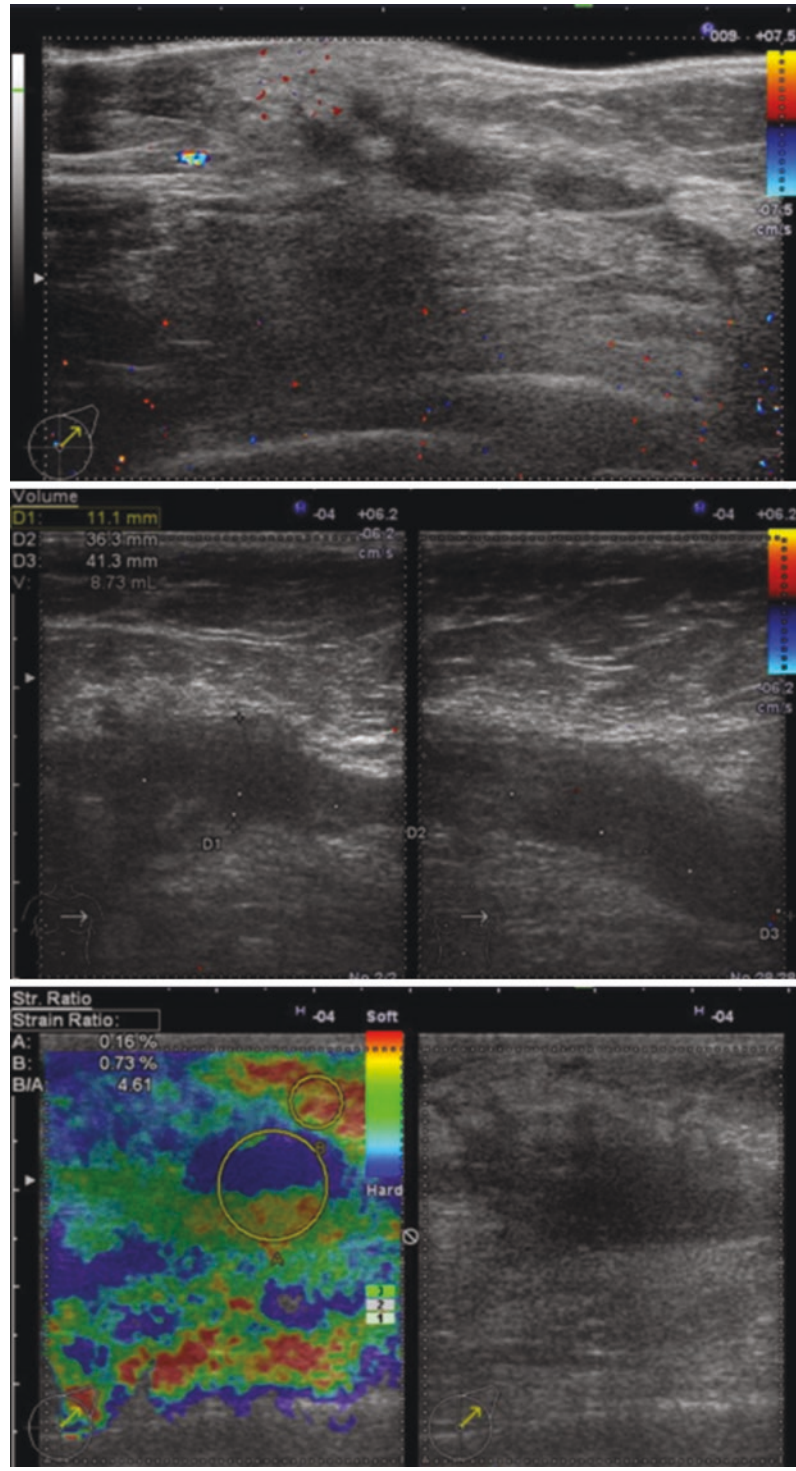

Fig. 8.25 Benign scar in a 38-year-old patient with conservatory surgery for breast cancer: the absence of a salient suspect vasculature (**a** and **b**) and the BGR score (**c**) are the most significant findings for the differential diagnosis with a malignancy, suggested by the hypoechoic mass with ductal connection and spiculated shape

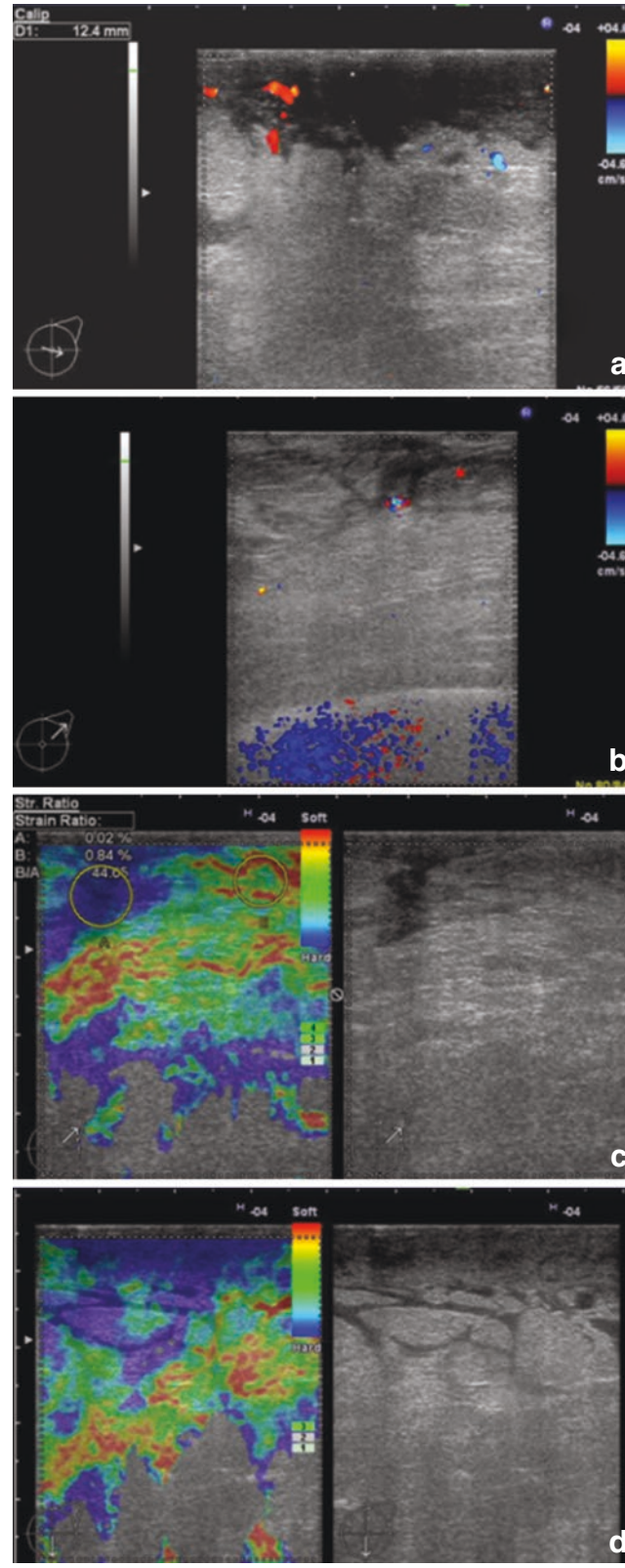

Fig. 8.26 Malignant breast scar in the left upper-outer quadrant with proliferative extension to the nipple-areolar complex in a 62-year-old patient: superficial mass with accentuate hypoechogenicity and multipolar new formation vasculature (**a** and **b**); the high strain with score 5 Ueno and FLR up to 44.65 (**c**) and lymphedema in the lower quadrants demonstrates increased hardness (**d**)

anatomical-functional unit of the mammary lobe, its complete excision reduces to minimal the risk of surgical seroma or hematoma, with esthetical and psychological best results (see the chapters about new surgical treatment of the breast cancer).

8.6 Differential Diagnosis of the Satellite Lymph Node Appearances

The study of the satellite lymph nodes by FBU is useful in all breast examinations, even in cases of normal breast findings, because there are other etiologies for abnormal lymph nodes, either systemic inflammatory processes (sarcoidosis), infectious diseases (bacterial lymphadenitis, tuberculosis, borreliosis), or malignancies (lymphoma, malignant melanoma, or lung, stomach, ovarian carcinomas). In some cases, there are other masses in the satellite areas, which must be differentiated from a metastatic lymph node: lipoma, sarcoma, seroma, aneurism, venous thrombosis, collagen vascular diseases, and miscellaneous (silicone implants, tattooing).

Mammography was the first technique of examination that visualized better in the MLO view the normal axillary lymph nodes (small, with oval shape and central lucency due to the fatty hilum/medullary) and the abnormal lymph nodes characterized by higher density, reduced or absent hilar fat, and a round, irregular, ill-defined shape with or without intra-nodal calcifications. Mammography may demonstrate abnormal axillary findings in cases without breast suspect findings, the so-called negative mammograms [38]; the breast cancer cannot be excluded, because the occult cancer to the radiological examination (missed cancers by mammography) may be found in screening mammograms about one in five breast cases, either in dense breasts or in small lesions, without microcalcification and stromal desmoplastic reaction [39]. However, the specificity of mammography for the axillary lymph nodes is low, and the sensibility is limited by the anatomical location, only the lowest axillary lymph nodes being accessible to the radiological examination, while the deeper ones and other stations (sub- and supraclavicular, internal mammary nodes) cannot be explored. The lymphadenography performed 24 h after injection of oil-soluble iodinated contrast agent or dynamic acquisition after water-soluble contrast is an invasive technique, with low accuracy for the completely invaded nodes, practically abandoned after US and CT development. A supplementary advantage has the FDG-PET as a noninvasive procedure that allows, within a single examination, the biological characterization of breast cancer and viewing of the entire body; however, FDG-PET has a lower sensibility than the sentinel lymph node biopsy in detecting the micro-metastasis [40].

MRI should be the best method of examination, because all satellite nodal stations can be visualized and characterized; however, the specificity of the MRI remains unsatisfactory, and the number of biopsies increased. The accuracy of MRI is not adequate to obviate either the pretherapeutic or the post-neoadjuvant chemotherapy status of the axillary lymph nodes [41] and could not replace the sentinel node biopsy.

US is able to detect all satellite stations: axillary, sub- and supraclavicular, internal mammary, thoracic lateral chain, and lateral cervical and spinal chains. A normal lymph node demonstrates at US scanning a thin hypoechogenic cortex in the periphery interrupted by the hyperechogenic fatty hilum that continues with the central nodal area or the medullary zone; Doppler signal may be absent, or few vessels (artery and veins) may be demonstrated in the hilum with centrifugal orientation, but without extension to the normal cortex. The lymphatic vessels are not salient in mammography or imaging techniques, because of their thin structure and of the low velocity of the lymph; anatomically the afferent lymphatic vessels penetrate the node cortex, and the efferent enlarged vessel leaves the node by hilum.

US completed with Doppler and SE, as an equivalent to the FBU, is useful in the differential diagnosis of the benign from the malignant nodes: the largest size is not significant, but the ratio transverse to longitudinal diameter is normally under 0.50; the main diameter with role in the differential diagnosis is the transverse one (short axes) that has <10 mm for the axillary

benign nodes. Focal thickening with more hypoechoic texture of the node cortex is suspect of micro-metastases by the way of the afferent lymphatic vessels, and the presence of new formation cortical vessels with increased focal stiffness has great accuracy. The differential diagnosis with the benign adenomegaly includes the longer axis development; thin cortex even with undulated, microlobulated contour; large medullary area even with central hypoechoic aspect in benign reactive hystiocitosis (Fig. 8.27); reduced vasculature exclusively in the hilum; and a normal strain of score 1 or 2 Ueno or cortical BGR score significant for lymphedema. The axillary node hystiocitosis is usually present in chronic galactophoritis and is frequently described associated with breast cancers.

The abnormal malignant nodes tend to become more round because of the cortical thickening (Fig. 8.28), with increasing of the intracapsular pressure; this determines the obliteration of the central medullary area (hilar replacement) before increasing of the longitudinal axis of the involved node (Fig. 8.29); other descriptors mentioned in the literature such as unclear margins, node matting, and perinodal edema [42] are very rare, even in large, multiple metastases of the breast cancer. The peripheral flow and the transcapsular vessels seen on color Doppler represent one of the most significant descriptors for malignancy, but they are reduced or absent in necrotic nodes and after neoadjuvant chemotherapy or radiotherapy (Fig. 8.30); for an accurate diagnosis, the most authors recommend needle aspiration or biopsy

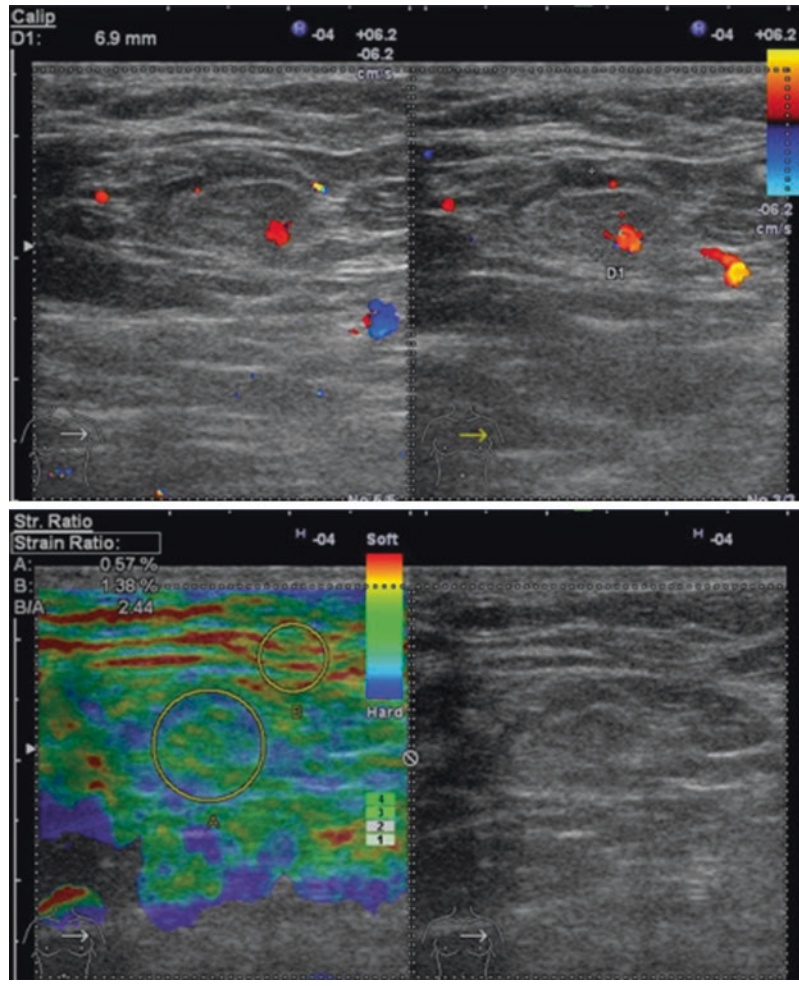

Fig. 8.27 Chronic lymphadenitis-type benign reactive histiocytosis: thin cortex, normal bloody vessels in the hilum, and moderate hypoechoic central area of the medullary (*upper* image); complementary benign SE type score 2 Ueno is reinforcing the diagnosis (*lower* image)

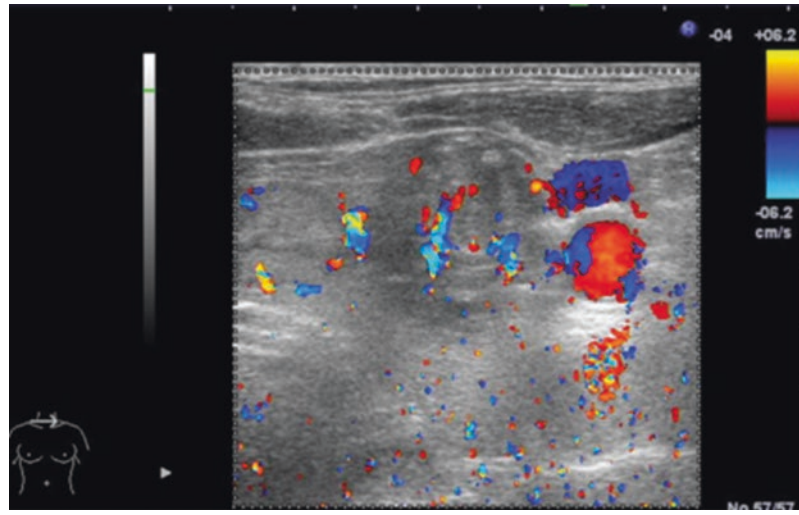

Fig. 8.28 Malignant left supraclavicular lymph node in a 58-year-old patient with left breast cancer; differential diagnosis with other metastasis (Virchow-Troisier sign), other tumors

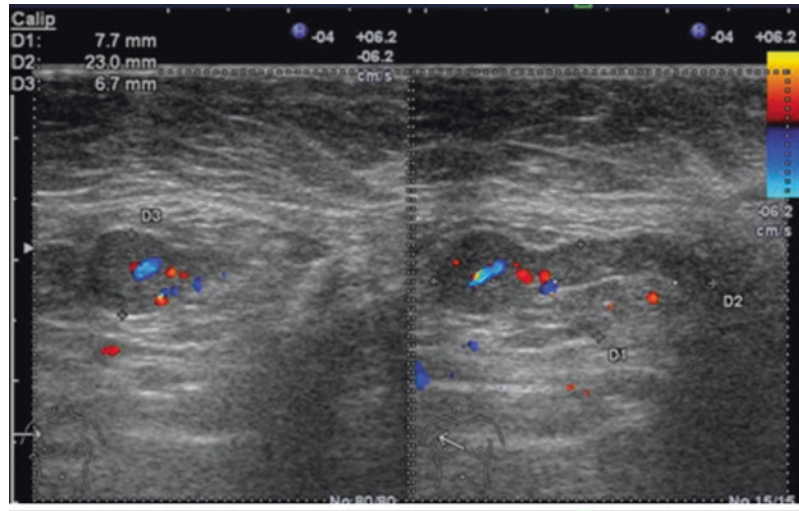

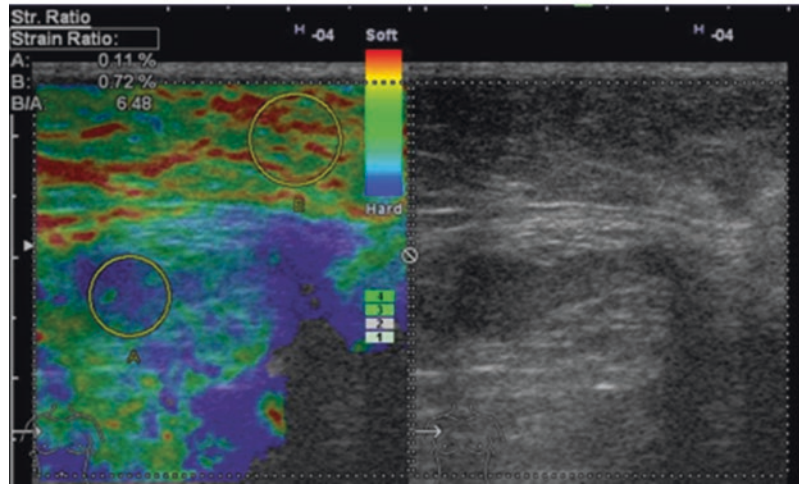

Fig. 8.29 Remnant lymph node with partial metastasis in a 65-year-old patient, with late recurrence 1 year after complex treatment, demonstrates cortical vasculature concordant with the focal thickening and increased strain

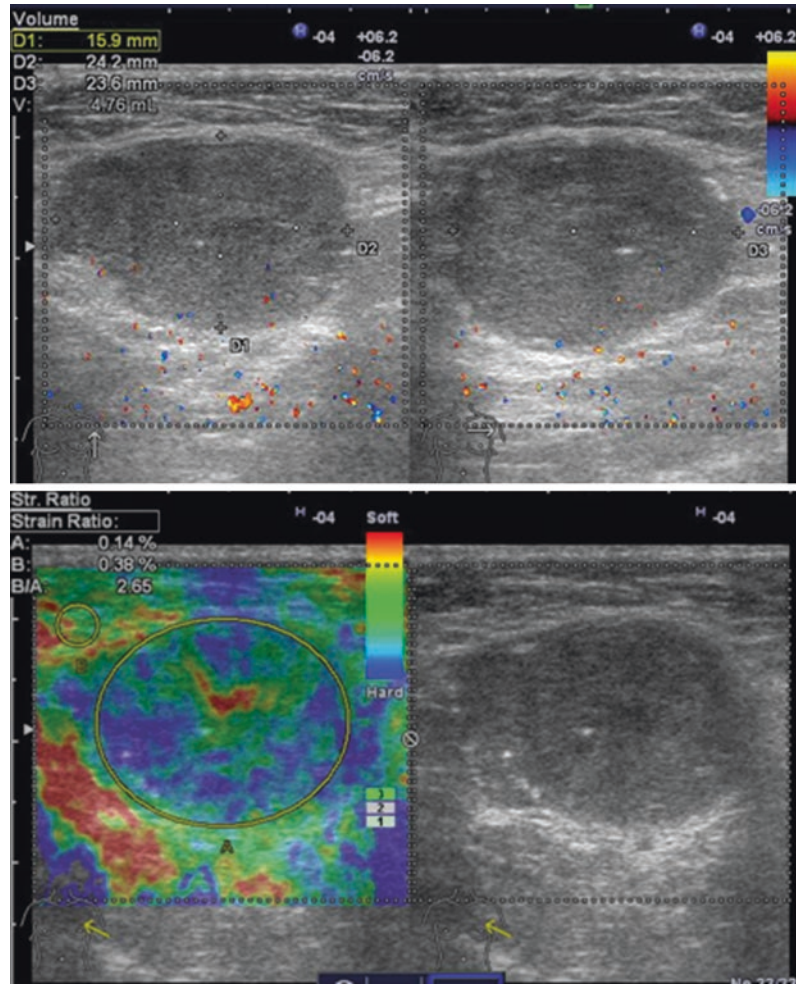

Fig. 8.30 Malignant left axillary lymph node after radiotherapy: the absence of pathological vasculature and the score 2 Ueno with FLR up to 2.65 are significant for the therapeutical response. Differential diagnosis with any benign findings

performed under US guidance. The Doppler examination is however a good tool of evaluation of the response to the therapy; when adding the SE, the accuracy is over 95% [35], because even in micro-metastases or in necrotic nodes, it presents a focal/global increasing of the SE score (3, 4, or 5 Ueno), with proportional increasing of the FLR; by opposite, the inflammatory nodes demonstrate the score 2 Ueno or BGR in the cases with edema or benign necrosis, associated with increased hilar vasculature. Some cancers with extensive microcalcifications determine calcifications in the node metastases, with very high FLR value, concordant with the CT aspect.

These descriptors of lymphadenopathy on FBU based on the vasculature and SE are more specific than the size, shape, internal architecture, or posterior effects and have an overall accuracy superior than those demonstrated by mammography, MRI, or FDG-PET, with reduced cost-benefit ratio. When present on FBU, the suspect axillary lymph nodes are correlated with the CA 15-3 level and the pathological reports; however, in practice usually a smaller number of suspect lymph nodes than the pathological report are found, which means not all micro-metastases could yet be diagnosed by noninvasive methods.

FBU is useful in the follow-up of treated cancers especially in detecting of the remnant ipsilateral axillary lymph nodes that could demonstrate late salient metastases and of the contralateral malignant lymph nodes that may appear after several years.

The differential diagnosis with other masses in the satellite areas of the breast cancer is based on the shape, size, anatomical reports, internal

structure, vasculature, and strain; before any biopsy, the imaging diagnosis for particular cases could be completed with MRI or MDCT for the characterization of the local extension and the analysis of the bone integrity.

References

1. Stavros AT, Thickman D, Rapp CL, Dennis MA, Parker SH, Sisney GA. Solid breast nodules: use of sonography to distinguish between benign and malignant lesions. Radiology. 1995;196:123–34.
2. Sala M, Salas D, Belvis F, et al. Reduction in false-positive results after introduction of digital mammography: analysis from four population-based breast cancer screening programs in Spain. Radiology. 2011;258(2):388–95. https://doi.org/10.1148/radiol.10100874.
3. Pisano ED, Gatsonis C, Hendrick E, et al. Diagnostic performance of digital versus film mammography for breast-cancer screening. N Engl J Med. 2005;353:1773–83.
4. Brem RF, Tabár L, Duffy SW, et al. Assessing improvement in detection of breast cancer with three-dimensional automated breast us in women with dense breast tissue: the SomoInsight study. Radiology. 2015;274(3):663–73. https://doi.org/10.1148/radiol.14132832.
5. Berg WA, Zhang Z, Lehrer D, et al. Detection of breast cancer with addition of annual screening ultrasound or a single screening MRI to mammography in women with elevated breast cancer risk. JAMA. 2012;307(13):1394–404. (ISSN: 1538-3598).
6. Teboul M, Halliwell M. Atlas of ultrasound and ductal echography of the breast (Relié). London: Blackwell Science Inc; 1995.
7. Teboul M. Practical ductal echography: guide to intelligent and intelligible Ultrasound imaging of the breast. Madrid: Saned Editors; 2003.
8. Tot T. Subgross morphology, the sick lobe hypothesis, and the success of breast conservation. Int J Breast Cancer. 2011;2011:634021 . 8 p. https://doi.org/10.4061/2011/634021.
9. Amy D. Lobar ultrasound of the breast. In: Tot T, editor. Breast cancer. London: Springer; 2010. https://doi.org/10.1007/978-1-84996-314-5_8.
10. Amy D, Durante E, Tot T. The lobar approach to breast ultrasound imaging and surgery. J Med Ultrasonics. 2015;42:331. https://doi.org/10.1007/s10396-015-0625-5.
11. Colan-Georges A. Atlas of full breast ultrasonography. New York, NY: Springer; 2016.
12. D'Orsi CJ, Sickles EA, Mendelson EB, Morvis EA, et al. ACR BI-RADS ® Atlas, breast imaging reporting and data system. Reston, VA: American College of Radiology; 2013.
13. Bamber JC, Sambrook M, Minassian H, Hill CR. Doppler studies of blood flow in breast cancer. In: Jellins J, Kobayashi T, editors. Ultrasonic examination of the breast. Chichester: John Wiley & Sons; 1983. p. 371–8.
14. Ramos IM, Taylor KJW, Kier R, Burns PN, Snower DP, Carter D. Tumor vascular signals in renal masses: detection with Doppler US. Radiology. 1988;168:633–7.
15. Shimamoto K, Sakuma S, Ishigaki T, Ishiguchi T, Itoh S, Fukatsu H. Hepatocellular carcinoma: evaluation with color Doppler US and MR imaging. Radiology. 1992;182:149–53.
16. Gasparini G, Weidner N, Bevilacqua P, et al. Tumor microvessel density, p53 expression, tumor size, and peritumoral lymphatic vessel invasion are relevant prognostic markers in node-negative breast carcinoma. J Clin Oncol. 1994;12:454–66.
17. Yang WT, Tse GMK, Lam PKW, et al. Correlation between color power Doppler sonographic measurement of breast tumor vasculature and immunohistochemical analysis of microvessel density for the quantitation of angiogenesis. J Ultrasound Med. 2002;21(11):1227–35.
18. Kedar RP, Cosgrove D, McCready VR, Bamber JC, Carter ER. Microbubble contrast agent for color Doppler US: effect on breast masses: work in progress. Radiology. 1996;198:679–86.
19. Van Esser S, Veldhuis WB, van Hillegersberg R, et al. Accuracy of contrast-enhanced breast ultrasound for pre-operative tumor size assessment in patients diagnosed with invasive ductal carcinoma of the breast. Cancer Imaging. 2007;7(1):63–8. https://doi.org/10.1102/1470-7330.2007.0012.
20. Kujiraoka Y, Ueno E, Yohno E, Morishima I, Tsunoda-Shimizu H. Incident angle of the plunging artery of breast tumors. In: Research and development in breast ultrasound. Tokyo: Springer; 2005. p. 72–5.
21. Christopher C. Ultrasound elastography of breast lesions. Ultrasound Clin. 2011;6:407–15. https://doi.org/10.1016/j.cult.2011.05.004.
22. Georgescu A, Bondari S, Manda A, Andrei E-M. The differential diagnosis between breast cancer and fibro-micro-cystic dysplasia by full breast ultrasonography-a new approach. Vienna: ECR; 2012. https://doi.org/10.1594/ecr2012/C-0167. EPOS™.
23. Stavros AT, Rapp LC, Parker HS. Breast ultrasound. Philadelphia, PA: Lippincott Williams & Wilkins; 2004.
24. Georgescu A, Enachescu V, Bondari A, et al. A new concept: the full breast ultrasound in avoiding false negative and false-positive sonographic errors. Vienna: ECR; 2011. https://doi.org/10.1594/ecr2011/C-0449.
25. Venta LA, Kim JP, Pelloski CE, et al. Management of complex breast cysts. Am J Roentgenol. 1999;173:1331–6.
26. Teboul M. Advantages of ductal echography (DE) over conventional breast investigation in the diagnosis of breast malignancies. Med Ultrason. 2010;12(1):32–42.

27. Tot T. The theory of the sick breast lobe and the possible consequences. Int J Surg Pathol. 2007;15(4):369–75. https://doi.org/10.1177/1066896907302225.
28. Tot T. The theory of the sick lobe. In: Tot T, editor. Breast cancer: a lobar disease. London: Springer; 2011. p. 1–18.
29. Holland R, Hendriks JH. Microcalcifications associated with ductal carcinoma in situ: mammographic-pathologic correlation. Semin Diagn Pathol. 1994;11(3):181–92.
30. Edmiston CE Jr, Walker AP, Krepel CJ, Gohr C. The nonpuerperal breast infection: aerobic and anaerobic microbial recovery from acute and chronic disease. J Infect Dis. 1990;162:695–9.
31. Graf O, Helbich TH, Hopf G, Graf C, Sickles EA. Probably benign breast masses at US: is follow-up an acceptable alternative to biopsy? Radiology. 2007;244:87–93.
32. Hertl K, Marolt-Musik M, Kocijancic I, et al. Haematomas after percutaneous vacuum assisted breast biopsy. Ultraschall Med. 2007;30:33–6.
33. Jackman RJ, Nowels KW, Rodriguez-Soto J, et al. Stereo-tactic, automated, large core needle biopsy of nonpalpable breast lesions: false-negative and histologic underestimation rates after long-term follow-up. Radiology. 1999;210:799–805.
34. Nielsen M, Christensen L, Andersen J. Radial scars in women with breast cancer. Cancer. 1987;59(5):1019–25.
35. Georgescu AC, Andrei ME. Full breast ultrasonography as follow-up examination after a complex treatment of breast cancer. Vienna: ECR; 2015. https://doi.org/10.1594/ecr2015/C-0266.
36. Freedman GM, Fowble BL. Local recurrence after mastectomy or breast-conserving surgery and radiation. Oncology. 2000;14(11):1561–81. discussion 1581-2, 1582-4.
37. Dolphin G. The surgical approach to the “sick lobe”. In: Francescatti DS, Silverstein MJ, editors. Breast cancer: a new era in management. New York, NY: Springer; 2014. p. 113–32.
38. Görkem SB, O’Connell AM. Abnormal axillary lymph nodes on negative mammograms: causes other than breast cancer. Diagn Interv Radiol. 2012;18:473–9.
39. American Cancer Society. Mammograms and other breast imaging tests. 2014. Last Medical Review: 12/8/2014 Last Revised: 4/25/2016; 2014 Copyright American Cancer Society.
40. Crippa F, Gerali A, Alessi A, Agresti R, Bombardieri E. FDG-PET for axillary lymph node staging in primary breast cancer. Eur J Nucl Med Mol Imaging. 2004;31(Suppl 1):S97–102.
41. Javid S, Segara D, Lotfi P, Raza S, Golshan M. Can breast MRI predict axillary lymph node metastasis in women undergoing neoadjuvant chemotherapy. Ann Surg Oncol. 2010;17(7):1841–6. https://doi.org/10.1245/s10434-010-0934-2.
42. Misselt PN, Glazebrook KN, Reynolds C, et al. Predictive value of sonographic features of extranodal extension in axillary lymph nodes. J Ultrasound Med. 2010;29:1705–9.